2018-09-14

Characterization of Proteoglycan 4 Supramolecular Structure and its Effect on Lubricating Function

Martens, Kayla

UNIVERSITY OF CALGARY

Characterization of Proteoglycan 4 Supramolecular Structure and its Effect on Lubricating Function

By

Kayla Martens

A THESIS

SUBMITTED TO THE FACULTY OF GRADUATE STUDIES

IN PARTIAL FULFILMENT OF THE REQUIREMENTS FOR THE

DEGREE OF MASTER OF SCIENCE

GRADUATE PROGRAM IN BIOMEDICAL ENGINEERING

CALGARY, ALBERTA

SEPTEMBER, 2018

Abstract

Proteoglycan 4 (PRG4) is a mucin-like glycoprotein that is a key synovial fluid constituent, functioning as a cartilage boundary lubricant. PRG4 has been suggested to exist as a supramolecular structure. The objectives of this thesis were to (1) characterize the supramolecular structure of recombinant human PRG4 (rhPRG4) and its dependency on concentration, (2) elucidate the molecular forces underlying the formation of the supramolecular structure, and (3) assess the lubricating ability of the supramolecular structure. rhPRG4's ability to form a supramolecular structure and reduce friction was concentration dependent. Arginine (0.2M) disrupted the formation of the supramolecular structure of rhPRG4 and diminished its lubricating ability. Conversely, 20 mM calcium enhanced the formation of rhPRG4 supramolecular structure and enhanced its lubricating ability. These results suggest non-covalent interactions mediate rhPRG4's supramolecular structure, shown here to exist for the first time, which in turn is a functionally (lubrication) determinant property.

Acknowledgements

I would like to thank my supervisor, Dr. Tannin Schmidt for allowing me the opportunity to study under your guidance and for always being available to chat, as well as the opportunity to present my work at an international conference.

Thank you to my co-supervisor, Dr. Justin MacCallum, and my committee members Dr. Darren Derksen, and Dr. Arindom Sen for taking the time to listen to me present my work and for giving me suggestions on how to improve. I would also like to thank Dr. Roman Krawetz and Dr. Kenneth Ng for taking the time to read my thesis and serve on my examination committee.

Finally, thank you to the members of the Schmidt lab group, especially Dr. Suresh Regmi for your patience and time spent teaching me lab techniques.

Table of Contents

Abstract ..... **i**

Acknowledgements ..... **ii**

List of Figures ..... **v**
List of Symbols, Abbreviations and Nomenclature ..... **vii**

Chapter 1: Introduction **1**
1.1 Synovial Joints **1**
1.1.1 Articular Cartilage 2
1.1.2 Synovial Fluid (SF) 5
1.1.3 Osteoarthritis 6
1.1.3.1 Synovial Fluid in Injury and Disease 7
1.1.3.2 Current Treatment Options 8
1.2 Modes of Lubrication **9**
1.2.1 Synovial Joint Lubrication 10
1.3 Analysis of Lubrication **12**
1.4 Proteoglycan 4 (PRG4) **13**
1.4.1 Structure – Function Relationship 14
1.4.2 PRG4 in Osteoarthritis 19
1.4.3 Recombinant Human PRG4 (rhPRG4) 21
1.5 Supramolecular Chemistry **21**
1.5.1 Hydrogen Bonding 21
1.5.2 Hydrophobic Interactions 22
1.5.3 Electrostatic Interactions 22
1.5.4 Cation – π Interactions 22
1.6 Calcium Interactions with Proteins **23**
1.7 Arginine Interactions with Proteins **24**
1.8 PRG4 Interaction with Calcium and Arginine **26**
1.9 Hypothesis and Aims **26**

Chapter 2: Methods **28**
2.1 rhPRG4 Sample Preparation **28**
2.2 Gel Electrophoresis and Western Blotting **28**
2.2.1 Background 28
2.2.2 Analysis 29
2.2.2.1 SDS-PAGE 29
2.2.2.2 Native PAGE 30
2.3 Dynamic Light Scattering **31**
2.3.1 Background 31
2.3.2 Analysis 32
2.3.3 Statistical Analysis 33
2.4 Friction Testing **33**
2.4.1 PDMS-Glass Tribology Tests 33
2.4.1.1 Background 33
2.4.1.2 Tribology Tests 35
2.4.1.3 Tribology Test Sequences 36

2.4.1.4 Statistical Analysis 37
2.4.2 Cartilage Boundary Lubrication Tests 37
2.4.2.1 Background 37
2.4.2.2 Sample Preparation 39
2.4.2.3 Lubrication Tests 39
2.4.2.4 Lubrication Test Sequences 42
2.4.3 Statistical Analysis 42
2.4.3.1 Cartilage-Cartilage Friction Testing 42

Chapter 3: Results 44
3.1 Effect of Concentration on rhPRG4 Size and Lubricating Ability at a PDMS-Glass Interface 44
3.1.1 Western Blotting 44
3.1.2 Dynamic Light Scattering 45
3.1.3 Tribology Measurements 47
3.2 Effect of Buffer on rhPRG4 Size/Structure and Lubricating Ability at a PDMS-Glass Interface 49
3.2.1 Western Blotting 49
3.2.2 Dynamic Light Scattering 50
3.2.3 Tribology Measurements 52
3.2.3.1 Lubricating Ability of PBS+rhPRG4 at a PDMS-Glass Interface Compared to PBS Alone 52
3.2.3.2 Lubricating Ability of Arginine+rhPRG4 at a PDMS-Glass Interface Compared to Arginine Alone 55
3.2.3.3 Lubricating Ability of Calcium+rhPRG4 at a PDMS-Glass Interface Compared to Calcium Alone 57
3.3 Effect of Buffer on Lubricating Ability of rhPRG4 at a Cartilage-Cartilage Interface 59
3.3.1 Cartilage Boundary Lubricating Ability of PBS+rhPRG4 Compared to PBS Alone 59
3.3.2 Cartilage Boundary Lubricating Ability of Arginine+rhPRG4 Compared to Arginine Alone 60
3.3.3 Cartilage Boundary Lubricating Ability of Calcium+rhPRG4 Compared to Calcium Alone 62

Chapter 4: Discussion 66
4.1 Effect of Concentration on rhPRG4 Size and Lubricating Ability 66
4.2 Effect of Arginine on rhPRG4 Size and Lubricating Ability 69
4.3 Effect of Calcium on rhPRG4 Size and Lubricating Ability 72
4.4 Limitations 75

Chapter 5: Conclusions 78
5.1 Summary of Findings 78
5.2 Future Work 80

References 84
Appendix 90

List of Figures

Figure 1-1. Schematic representation of a synovial joint depicting key structures. Adapted from [4]. 2

Figure 1-2. Cross-sectional schematic of healthy articular cartilage demonstrating the cellular organization in each zone (**A**) and the collagen fiber organization (**B**). Adapted from [5]. ... 5

Figure 1-3. Stribeck curve (red) showing friction coefficient (μ) as a function of shear velocity and fluid viscosity with corresponding film thickness (blue) in the boundary, mixed, and hydrodynamic lubrication regimes. Adapted from [17]. 10

Figure 1-4. Stribeck curve demonstrating the synergistic ability of lubricin and hyaluronate to function as an effective lubricant compared to hyaluronate alone. Adapted from [19]. 12

Figure 1-5. Schematic of a PRG4 monomer depicting the central mucin-like domain and the globular N- and C-termini. Adapted from [41]. 15

Figure 1-6. Kinetic $<\mu_{kinetic,\ Neq}>$ of coefficient of friction of PRG4Multi- and PRG4Multi+ at 450 μg/mL. * indicates $p < 0.05$. Adapted from [39]. 18

Figure 1-7. Schematic representation of adsorption of PRG4 on (**a**) hydrophobic and (**b**) hydrophilic surfaces. Adapted from [38] 19

Figure 2-1. Schematic illustration of tribological set-up of three cylindrical samples with a spherical probe. Adapted from [22]. 35

Figure 2-2. Schematic illustration of in vitro cartilage-cartilage boundary lubrication test. Osteochondral blocks were harvested from the patellofemoral groove of bovine stifle joints (**A**) and annulus (ann) and core samples were prepared (**B**). Samples were incubated at 4 ℃ for 24 hr in test lubricant (**C**) prior to testing (**D**). Adapted from [25]**.** 41

Figure 3-1. Native PAGE (**A**) and SDS-PAGE (**B**) western blot of rhPRG4 at concentrations of 50, 150, 450, and 1200 μg/mL with mAb 9G3. 44

Figure 3-2. Number distribution (%) (**A**) and intensity distribution (%) (**B**) versus particle size (hydrodynamic diameter, nm) of rhPRG4 at concentrations of 50, 150, 450, 1200 μg/mL (N = 3) and Z-average (**C**) demonstrating the mean $\pm$ SEM size of particles in solution increasing with concentration. 47

Figure 3-3. Stribeck curve of $\mu_{kinetic}$ of rhPRG4 at concentration of 50, 150, 450, and 1200 μg/mL at velocities of 0.01 – 1000 mm/s, showing a decrease in $\mu_{kinetic}$ with increasing rhPRG4 concentration (**A**) (N = 3). $\mu_{kinetic}$ was significantly decreased with increasing rhPRG4 concentration compared to PBS at a velocity of 0.398 mm/s (**B**). * denotes $p < 0.05$. 48

Figure 3-4. Western blot of rhPRG4 (450 μg/mL) in PBS, Arginine (0.2 M), and Calcium (20 mM) with mAb 9G3 (**A**) and Anti-PRG4 Ab LPN (**B**). 50

Figure 3-5. Number distribution (%) (**A**) and intensity distribution (%) (**B**) versus particle size (hydrodynamic diameter, nm) of rhPRG4 (450 μg/mL) in PBS, Arginine (0.2 M), and calcium (20 mM) (N = 3). The Z-average showing the average hydrodynamic size of particles in solution was significantly different in Calcium+rhPRG4 compared to PBS+rhPRG4 and Arginine+rhPRG4 (**C**). * denotes $p < 0.05$. 52

Figure 3-6. Stribeck curve showing $\mu_{kinetic}$ of PBS, PBS+rhPRG4(150 μg/mL), and PBS+rhPRG4(450 μg/mL) at velocities of 0.01 – 1000 mm/s (**A**) (N = 3). $\mu_{kinetic}$ was significantly decreased upon addition of rhPRG4 compared to PBS at velocities of 0.398 and 3.98 mm/s (**B**). * denotes $p < 0.05$. 54

Figure 3-7. Stribeck curve of $\mu_{kinetic}$ of Arginine, Arginine+rhPRG4(150 μg/mL), and Arginine+rhPRG4(450 μg/mL) at velocities of 0.01 – 1000 mm/s (**A**) (N = 3). $\mu_{kinetic}$ increased upon addition of rhPRG4 compared to Arginine at velocities of 0.398 and 3.98 and mm/s (**B**). 56

Figure 3-8. Stribeck curve showing $\mu_{kinetic}$ of Calcium, Calcium+rhPRG4(150 μg/mL), and Calcium+rhPRG4(450 μg/mL) at velocities of 0.01 – 1000 mm/s (**A**) (N = 3). $\mu_{kinetic}$ was significantly decreased upon addition of rhPRG4 to Calcium compared to Calcium alone at velocities of 0.398 and 3.98 mm/s (**B**). * denotes $p < 0.05$ 58

Figure 3-9. Static ($\mu_{static,Neq}$) (**A**) and kinetic ($<\mu_{kinetic,Neq}>$) at Tps = 1.2 s (**B**) friction coefficients of PBS, PBS+rhPRG4 and SF with rhPRG4 preparations at 450 μg/mL (N = 4). * denotes $p < 0.05$. 60

Figure 3-10. Static ($\mu_{static,Neq}$) (**A**) and kinetic ($<\mu_{kinetic,Neq}>$) at Tps = 1.2 s (**B**) friction coefficients of Arginine, Arginine+rhPRG4 and SF with rhPRG4 preparations at 450 μg/mL (N = 4). 62

Figure 3-11. Static ($\mu_{static,Neq}$) (**A**) and kinetic ($<\mu_{kinetic,Neq}>$) at Tps = 1.2 s (**B**) friction coefficients of Calcium, Calcium+rhPRG4 and SF with rhPRG4 preparations at 450 μg/mL (N = 4). * denotes $p < 0.05$. 64

Figure 4-1. Kinetic $<\mu_{kinetic,\ Neq}>$ coefficient of friction at Tps = 1.2 s of (**A**) buffer solutions and (**B**) buffers with rhPRG4 (450 μg/mL) added …… 69

List of Symbols, Abbreviations, and Nomenclature

μ	Coefficient of friction μ
$\mu_{static,Neq}$	Static coefficient of friction calculated using equilibrium axial load
$<\mu_{kinetic,Neq}>$	Kinetic coefficient of friction calculated using equilibrium axial load
π	pi
η	Viscosity
9G3	Anti-PRG4 antibody, mucin domain
Ab	Antibody
ANOVA	Analysis of variance
ACL	Anterior cruciate ligament
C – terminal	Carboxy terminal
$CaCl_2$	Calcium chloride
CACP	Camptodactylyl-arthropathy-coxa vara-pericarditis
cDNA	Complimentary deoxyribonucleic acid
CHO	Chinese hamster ovary
COX-II	Cyclooxygenase II
D	Diffusion coefficient
d_H	Hydrodynamic diameter
DLS	Dynamic light scattering
ECM	Extracellular matrix
F	Friction force

Fe^{2+}	Iron
GAG	Glycosaminoglycan
HA	Hyaluronan
HsDNK	*Halobacetrium salinus* nucleoside disphosphate kinase
HMW	High molecular weight
HPLC	High performance liquid chromatography
HIC	Hydrophobic interaction chromatography
IA	Intraarticular
IgG	Immunoglobulin G
IL-1	Interleukin-1
IL-6	Interleukin-6
k	Boltzmann's constant
LGP-I	Lubricating Glycopeptide-I
LPN	Anti-PRG4 antibody, C-terminal
mAb	Monoclonal anti-body
MALLS	Multi-angle light scattering
Mg^{2+}	Magnesium
MMP	Matrix metalloprotein
MSF	Megakaryocyte stimulating factor
MW	Molecular weight
N	One test replicate
N-terminal	Amino terminal

NSAID	Non-steroidal anti-inflammatory drug
OA	Osteoarthritis
PAGE	Polyacrylamide gel electrophoresis
PBS	Phosphate buffered saline
PCS	Photon correlation spectroscopy
PDMS	Polydimethylsiloxane
PEX	Hemopexin
PRG4	Proteoglycan 4
PRG4Multi+	PRG4 Multi enriched
PRG4Multi-	PRG4 Multi deficient
R_i	Inner radius
R_o	Outer radius
rhPRG4	Recombinant human PRG4
s	Seconds
SAPL	Surface active phospholipids
SDS-PAGE	Sodium dodecyl sulfate polyacrylamide gel electrophoresis
SEM	Standard error of the mean
SEC	Size exclusion column
SF	Synovial fluid
SMB	Somatomedin B
SZP	Superficial zone protein
T	Absolute temperature

TGF-β1	Transforming growth factor beta- 1
Tps	Pre-sliding duration
W	Applied load

Chapter 1: Introduction

1.1 Synovial Joints

There are three types of joints in the human body: fibrous, cartilaginous, and synovial. Synovial, or diarthrodial joints allow for a wide range of motion between opposing bones. Some examples of this type of joint are the shoulder, hip, elbow, and knee. Synovial joints are enclosed by a fibrous capsule, which is typically reinforced by tendons and ligaments. These tendons and ligaments provide stability to the joint, maintain proper relative positions of bones during movement, and transmit muscle forces [1]. The inner surfaces of the joint capsule are lined with a metabolically active tissue called the synovium, or synovial membrane. The synovium creates synovial fluid and mediates exchange of nutrients and waste between blood and the joint. The bone ends in synovial joints are lined with a thin layer of articular cartilage, which along with the synovium forms the joint cavity. Together, the synovial fluid, articular cartilage, and supporting bone form the synovial joint (**Figure 1-1**), which provides a smooth, nearly frictionless [1] bearing system in a normal healthy body, with coefficient of friction values ranging from ~ 0.0005 – 0.04 [2]. These joints are subject to a wide range of loading conditions, yet under normal circumstances, the cartilage surfaces undergo little wear and tear [3]. Due to these wide range of conditions, synovial joints must be able to function effectively under high loads and stresses, and low operating speeds [3]. This requires efficient lubrication to minimize friction and wear of cartilage in the joint. Breakdown of cartilage induced by biochemical or biomechanical means may lead to joint disease such as arthritis [3].

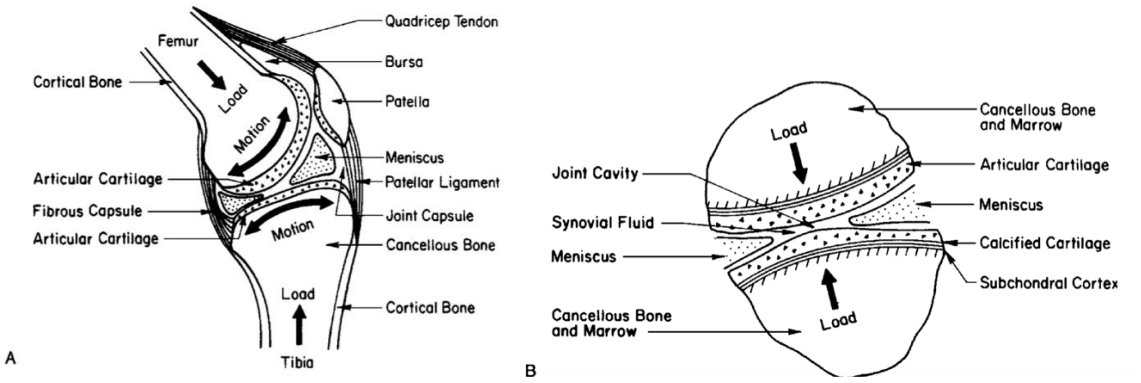

Figure 1-1. Schematic representation of a synovial joint depicting key structures. Adapted from [3].

1.1.1 Articular Cartilage

Articular cartilage is a specialized connective tissue lining the articulating surfaces of bone in diarthrodial joints whose main function is to provide a smooth surface for articulation and to facilitate transmission of loads with a low coefficient of friction [4]. It is avascular, aneural, and alymphatic, and therefore has a limited ability to heal and repair itself [5]. Articular cartilage is 2 – 4 mm thick and composed of a dense extracellular matrix (ECM) embedded with specialized cells known as chondrocytes [4][6]. The ECM primarily consists of tissue fluid and structural macromolecules which gives cartilage its form and stability, and is attributed to the biomechanical function of cartilage [7]. The interaction of the tissue fluid and structural macromolecules are responsible for the mechanical properties of cartilage [7]. The tissue fluid is ~ 80% water and contains gases, small proteins, metabolites, as well as a high concentration of cations to balance the negatively charged proteoglycans [5]. There are three main structural macromolecules in the ECM, collagen, proteoglycans, and non-collagenous proteins. Collagen makes up ~ 60% of cartilage and creates a meshwork that gives cartilage its form and tensile strength [5]. Proteoglycans and non-collagenous proteins make up ~ 25-35 and ~ 15-20% of cartilage

respectively, and bind to the collagen frame or become trapped within it [5]. There are multiple distinct types of collagen in articular cartilage but Type II accounts for 90-95% and forms the cross-linked framework [5]. Type IX collagen helps to bind together the collagen fiber meshwork and help facilitate interactions with other ECM components. The inter- and intramolecular cross-linkages contribute to the mechanical properties of collagen and provide cartilage with its tensile properties. Proteoglycans are made up of a protein core substituted with glycosaminoglycan (GAG) chains [8]. The most abundant proteoglycan is aggrecan, which is a highly negative brush-like macromolecule [8]. Aggrecan becomes entrapped in the porous collagen network and binds non-covalently to a long-chain GAG, hyaluronan (HA) and is stabilized by a non-collagenous protein [8]. Multiple aggrecan molecules can bind to a single HA resulting in aggrecan aggregates [8]. The formation of these aggregates helps anchor proteoglycans within the matrix, preventing displacement during deformation of the cartilage, and helping to organize and stabilize proteoglycans and the collagen meshwork [5]. This creates a gel-like structure that contributes to important mechanical properties of cartilage such as, osmotic swelling pressure, hydraulic permeability, and resistance to compressive and shear deformation [8].

The main cell type in articular cartilage is chondrocytes. These cells are metabolically active and contribute to the development, maintenance, and repair of the ECM [8] by synthesizing collagen, proteoglycans, and non-collagenous proteins [5]. The size and shape of chondrocytes vary depending on the region of articular cartilage in which they are located [5]. Each chondrocyte creates a specialized microenvironment that traps the chondrocyte within its own matrix preventing migration to other areas of the cartilage [7]. These cell sense changes in composition of the ECM due to degradation of macromolecules and respond by synthesizing new macromolecules ensuring turnover and ongoing remodeling of the ECM. Chondrocytes have

limited ability to replicate, which contributes to the limited healing capacity of articular cartilage.

The structure of articular cartilage is critical to its function and mechanical properties. It is divided into four zones: superficial, middle, deep, and calcified (**Figure 1-2A**). The superficial zone is the outermost zone that protects the underlying zones from shear stresses and accounts for 10-20% of cartilage thickness [4]. The collagen fibers in this zone are Type II and IX and are tightly packed and parallel to the articular surface (**Figure 1-2B**) [4]. This layer contains many flattened chondrocytes and its integrity is important in the protection and maintenance of deeper layers. This zone is responsible for most of the tensile strength of cartilage, which enables it to resist shear, tensile, and compressive forces from articulation [4]. The middle zone accounts for 40-60% of total cartilage thickness and contains proteoglycans and thick collagen fibrils [4]. Collagen is organized obliquely and the chondrocytes are spherical and lower in density than the superficial zone. The deep zone makes up ~ 30% of cartilage thickness with chondrocytes in a columnar orientation parallel to collagen [4]. The deep zone provides the greatest resistance to compressive forces with collagen fibrils arranged perpendicular to the articular surface. This layer contains the largest collagen fibers, lowest water content, and highest proteoglycan content. The calcified zone helps secure the cartilage to bone by anchoring the collagen fibers from the deep zone to the subchondral bone. In this zone there is little cell population and chondrocytes are hypertrophic [4].

Each zone further consists of three regions: pericellular, territorial, and interterritorial. The pericellular region is a thin layer next to the cell membrane and completely surrounds the chondrocyte [5]. It is mainly composed of proteoglycans, glycoproteins and other noncollageous proteins [4]. The territorial region surrounds the pericellular region, and is composed mainly of collagen fibrils forming a network around cells [4][5]. This region helps protect chondrocytes from

mechanical stresses and may contribute to the resiliency of the cartilage and its ability to withstand large loads [4]. The interterritorial region contains randomly oriented bundles of large collagen fibers, and is abundant in proteoglycans [4][5]. This region is the largest of the three and contributes to the biomechanical properties of cartilage.

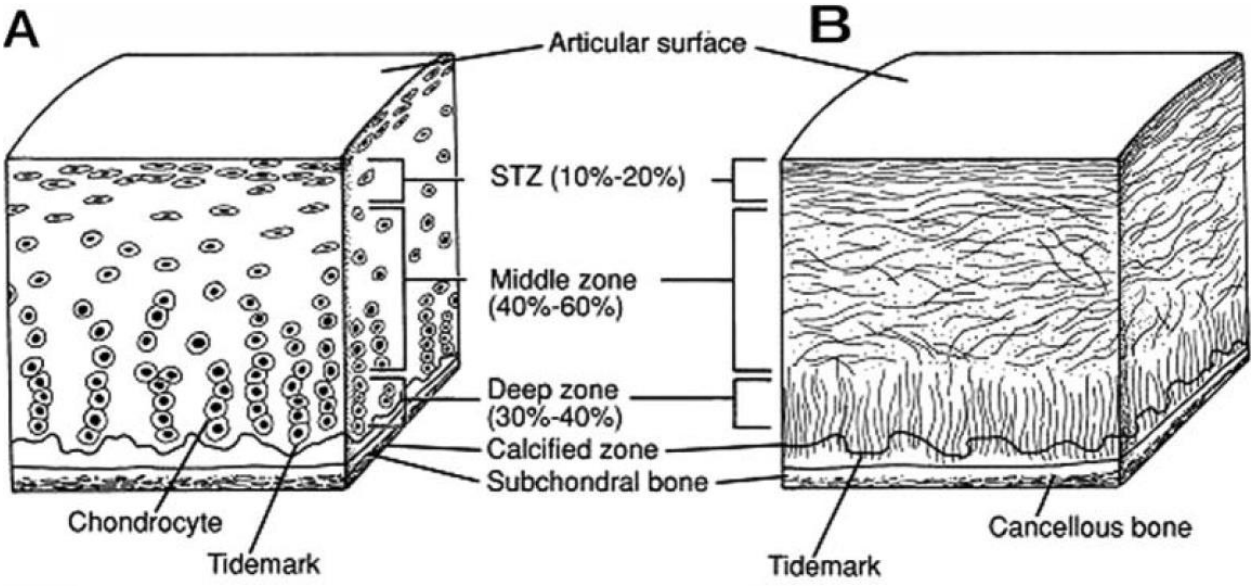

Figure 1-2. Cross-sectional schematic of healthy articular cartilage demonstrating the cellular organization in each zone (**A**) and the collagen fiber organization (**B**). Adapted from [4].

1.1.2 Synovial Fluid (SF)

Synovial fluid (SF) is a viscous, ultrafiltrate of plasma that is concentrated in synovial joints via filtration through the semi-permeable synovial membrane. SF is present in volumes of 0.5 – 2 mL [6] in healthy knee joints and has biomechanical, metabolic, and regulatory functions. One main function is that of a biological lubricant that provides low-friction and low-wear properties to articulating cartilage surfaces. The molecules in SF that play a key role in its lubricating properties are proteoglycan 4 (PRG4), hyaluronan (HA), and surface-active phospholipids (SAPL) [9]. PRG4 is present at 0.05-0.35 mg/mL [9] and a molecular weight (MW) of ~ 230-460 kDa [2], HA is present at 1-4 mg/mL [9] and MW of ~ 0.5-1 and 6-7 MDa [10], and

SAPL is present at 0.1 mg/mL [9] and MW of ~ 73 kDa [2]. HA is extremely viscous and is a major determinant of SF viscosity [6] with higher MW HA being more viscous than low MWs. Synoviocytes in the synovium secrete PRG4 and are the major source of SAPL and HA [9]. PRG4 is also secreted by chondrocytes in the superficial layer of articular cartilage, and to a lesser extent, cells in the meniscus [9].

1.1.3 Osteoarthritis

Osteoarthritis (OA) is a degenerative joint disease characterized by the loss of articular cartilage. This loss of cartilage can lead to joint swelling, stiffness, and limitation of movement. OA is the most common type of arthritis in the USA, Europe, and Japan with a prevalence of 36 – 48 % of the population with an expected growth rate of 1.1 – 1.2 % per year [6]. The joints most frequently affected are the knees, hands, feet, and hips. Degeneration begins at the articular surface with the fissures penetrating the damaged cartilage eventually progressing to the subchondral bone. This is then followed by progressive loss of cartilage thickness. Changes in ECM composition are observed, initially as an increase followed by a dramatic decrease in proteoglycan synthesis [11], and a phase of increased ECM turnover with depletion of proteoglycans and collagen. Finally, severe damage and loss of the collagen network are observed. There is also an increase in hydration due to weakening of the collagen network and an increase in swelling pressure from the rise in proteoglycan content [11]. Proteoglycan loss and an increase in water content lead to a decrease in cartilage stiffness and increase in hydraulic permeability [11]. These changes cause a decrease in fluid pressurization in the interstitial fluid thereby impairing the normal load-bearing capacity of the interstitial fluid [11]. This causes a greater load exerted on the collagen-proteoglycan matrix, exposing the ECM to further damage [11]. A variety of cytokines, growth factors and proteases contribute to the breakdown of cartilage. Matrix metalloproteins (MMPs) play a key role in

cleavage of cartilage macromolecules, such as Type II collagen and aggrecan. It is possible that the products of matrix degradation themselves stimulate degradation, creating a positive feedback loop [6]. This feedback loop includes the production of IL-1, which stimulates degradation and anti-inflammatory and modulatory cytokines that contribute to cartilage anabolism. OA is a relatively non-inflammatory condition, however there can be some synovitis in the synovium, the degree of which may influence the development and progression of pathological changes.

1.1.3.1 Synovial Fluid in Injury and Disease

A deficiency in the lubricating system in synovial joints can contribute to erosion of articulating cartilage surfaces leading to OA. Usually, the mechanobiology of joints and SF creates a complex, low-friction, low-wear system that is in homeostasis. In arthritis, injury, and artificial joint failure there is increased friction and erosion of the articulating surfaces. This increase in friction is associated with an altered SF composition, specifically, a lower PRG4 concentration following acute joint injury [9]. HA and SAPL concentrations are also decreased in OA and HA is decreased in failure of artificial joints [9]. In addition to a decreased concentration of HA in OA, there is also an altered MW distribution in SF with a shift to lower MWs [10]. Joint injury and arthritis can also result in changes in SF cytokine concentrations, specifically transforming growth factor beta-1 (TGF-β1) and interleukin-1 (IL-1). These cytokines can have significant effects on lubricant secretion by chondrocytes and synoviocytes, with TGF-β upregulating PRG4 and HA secretion and IL-1 downregulating PRG4 and upregulating HA secretion [9][12]. Therefore, the altered chemical environment in injury and arthritis can have significant effects on lubricant secretion and subsequently, SF composition. The mechanisms that contribute to altered SF composition remain to be fully elucidated [9].

1.1.3.2 Current Treatment Options

OA is responsive to a local intraarticular (IA) treatment in addition to systemic treatment. Most efforts in the development of OA treatment have focused on systemic treatments, however these agents have a risk for systemic adverse effects in the cardiovascular and gastrointestinal systems as seen with most non-steroidal anti-inflammatory drugs (NSAIDs) and cyclooxygenase (COX) II inhibitors used in treatment of joint pain. OA is a chronic disease and therefore requires a drug suitable for chronic systemic treatment with minimal side effects, which presents a challenge. Current treatment for OA that is frequently used is injection of drugs directly into the affected joint which can achieve a desired therapeutic effect and minimizes systemic side effects. It also allows for the possibility to achieve appropriate drug concentration at the site of action and delivery of drugs with good efficacy but low bioavailability. There are some disadvantages with this form of treatment, a major one being the risk of infection, as well as the pain and discomfort a patient may experience receiving the injection. Another disadvantage with IA injections is the ability to accurately localize the injections, as recent studies have found that about one third of knee injections are inaccurately administered [6]. Finally, a major challenge with IA drug delivery is the short residence time of the injection in the joint due to rapid uptake of the drugs.

Glucocorticoid and HA formulations are currently clinically available for OA treatment. Glucocorticoid injections are widely used for symptomatic treatment, especially in the knee. Though there is evidence that glucocorticoid injections are effective, the benefits only last 1 – 4 weeks, and are therefore recommended for short-term treatment to decrease pain [6]. Hydrogel formulations of HA in water are also used for OA treatment. These formulations usually contain a low MW (0.5 – 1.5 MDa) HA; however one formulation, Synvisc ®, contains a cross-linked HA with a MW of 6 – 7 MDa [6]. Many clinical trials have been done to assess different HA

preparations, with a majority of studies finding that HA preparations are effective in reducing OA associated pain; however, there is no evidence of superiority of high MW preparations compared to low MW preparations [6]. In contrast to glucocorticoids, HA is a slowing acting drug with a delayed onset of 2 – 5 weeks after injection with benefits lasting six months up to one year [6]. Therefore, glucocorticoids and HA preparations should be considered as complementary therapies [6]. The disadvantages associated with the current treatment methods for OA emphasize the need for the development of sustained release formulations which would be effective for longer periods of time.

1.2 Modes of Lubrication

Friction is the resistance to motion between two surfaces in contact with one another and can typically be defined as:

$$F = \mu W$$

where F is the frictional force, μ is the coefficient of friction, and W is the applied load (N) [3]. In synovial joints it is important that friction remains low during joint movement to maintain overall joint health and function. SF provides lubrication to articular cartilage, providing the low-friction and low-wear properties that are characteristic of these joints. Lubrication in the presence of fluid generally occurs in one of three regimes: hydrodynamic lubrication, mixed lubrication or boundary lubrication. These lubrication regimes can be visualized on a Stribeck curve which shows coefficient of friction as a function of shear velocity and fluid viscosity (**Figure 1-3**). Hydrodynamic lubrication, also referred to as fluid-film lubrication, typically occurs at high speeds and low load [13][14]. In this type of lubrication surfaces are separated by a fluid film and load is transmitted via that thin lubricant layer [3][15] . Boundary lubrication occurs at low speeds and high load [13][14]. In this mode of lubrication, surfaces are usually in full contact with one another

with loads transmitted directly between the two surfaces [15][16]. This mode of lubrication relies on a boundary lubricant to adhere to the articulating surfaces and reduce friction [16]. Mixed lubrication occurs when both hydrodynamic and boundary lubrication are present. In mixed lubrication load is transmitted through both direct contact and a thin fluid film between the articulating surfaces [16].

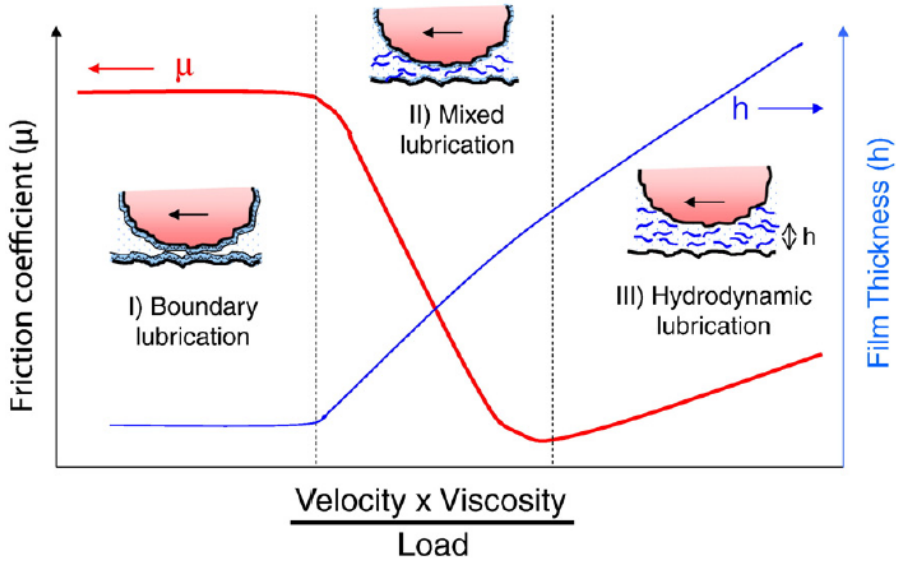

Figure 1-3. Stribeck curve (red) showing friction coefficient (μ) as a function of shear velocity and fluid viscosity with corresponding film thickness (blue) in the boundary, mixed, and hydrodynamic lubrication regimes. Adapted from [16].

1.2.1 Synovial Joint Lubrication

In contrast to the lubrication of hard, impermeable materials, articular cartilage lubrication is much more complicated. This is due to a number of factors including the relatively high compliance and permeability of the tissue, the presence of biolubricants in SF and at the tissue surface, and a dynamic tissue surface that is continually altered due to the mechanical and biochemical environment of the joint [14]. Though soft, permeable materials such as cartilage

undergo similar transitions in lubrication behavior, it has been suggested they do not achieve full hydrodynamic lubrication [17]. This deviation from the classic Stribeck curve is described by a elastoviscous transition that results from fluid pressurization and flow of fluid into and out of contacting surfaces [17]. Therefore, due to the complexity of cartilage it is generally accepted that multiple modes of lubrication occur within the joint. The biphasic nature of cartilage allows for hydrostatic fluid load support upon initial loading of the tissue [14]. This results in cartilage deformation and fluid flow into and from the interface due to tissue permeability, increasing elastohydrodynamic, squeeze film, boosted, and weeping mechanisms of lubrication [14]. As fluid load support is reduced, boundary mode lubrication becomes the dominant regime, in which cartilage-cartilage and cartilage-biomolecule interactions play a critical role in effective lubrication of the joint [14] . Boundary lubrication is achieved through lubricant localization at the cartilage surface. Due to the direct surface-to-surface contact in this regime high coefficients of friction compared to other modes of lubrication are achieved leading to greater wear and transfer of high shear stresses to articular cartilage [13]. Therefore, effective lubrication is critical to maintain healthy articular cartilage and prevent damage. The structure of cartilage itself helps to lower friction, but biochemical interactions at the tissue surface have been shown to reduce friction under boundary mode conditions [13]. Two SF constituents, HA and PRG4 have been shown to act synergistically to achieve effective boundary lubrication (**Figure 1-4**) [17][18]. The exact mechanism for this synergistic interaction remains to be fully understood [17].

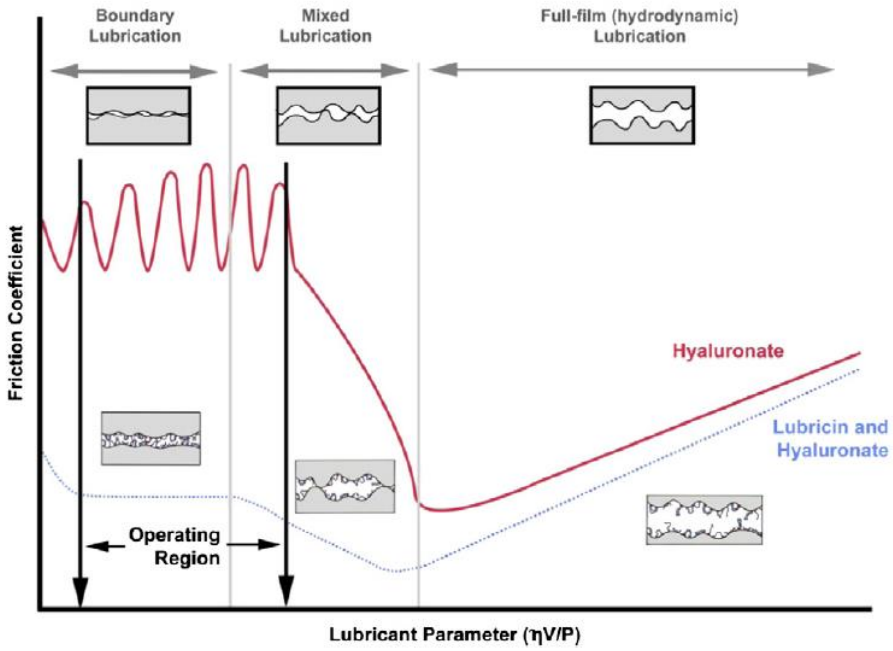

Figure 1-4. Stribeck curve demonstrating the synergistic ability of lubricin and hyaluronate to function as an effective lubricant compared to hyaluronate alone. Adapted from [18].

1.3 Analysis of Lubrication

Many methods and protocols have been developed to assess the lubricating ability of molecules such as PRG4. To analyze the lubricating ability of molecules in a whole joint, an ex vivo joint motion pendulum setup has successfully been utilized [19]. In this setup an animal knee joint is excised, with the femoral head fixed and the tibia allowed to move in a pendulum motion [19]. Though this setup is useful for measuring the coefficient of friction in the presence of multiple modes of lubrication and is the most physiologically relevant, it is not possible to isolate modes of lubrication. *In vitro* test setups have been developed, using a stationary area of contact, allowing for analysis of lubricant in boundary mode. In these test setups there are minimal ploughing friction losses since the surfaces remain in contact with one another, and fluid pressure effects are minimized due to slow velocities [20]. The interfaces used in these test setups vary with latex-glass, cartilage-glass, and cartilage-cartilage. The use of synthetic materials may not allow for all

physiological interactions of molecules and surface to occur, however these materials are readily available and easy to work with. The use of synthetic materials in a linear reciprocating test geometry, with migrating contact area, allows for classic Stribeck analysis, with varying velocity, fluid viscosity, and applied load, therefore allowing for isolation of a specific lubrication mode [21][22]. However, as mentioned previously, classical Stribeck analysis developed for hard, impermeable materials may not be appropriate for the soft and permeable cartilage. It has been observed previously that soft, permeable materials were unable to recreate a normal Stribeck curve [23]. A test using a cartilage-cartilage interface was developed allowing for analysis at a physiological interface and boundary mode lubrication [24]. Though preparation of cartilage samples can be challenging and may not enable comparison of results to a class Stribeck curve, it does allow for physiological interaction of lubricants with the cartilage surface, as well as allow for isolation of a boundary lubrication mode.

1.4 Proteoglycan 4 (PRG4)

Proteoglycan 4 (PRG4), also known as lubricin is a mucin-like glycoprotein synthesized and secreted by cells in articular joints including synoviocytes and superficial zone articular chondrocytes and found in SF [25]. PRG4 can be found throughout the body in various tissues other than SF such as the surface of tendons [26], pericardium [27][28], and the ocular surface [29].

In 1973, Swann et al fractioned bovine SF and discovered that the lubricating quality of SF was not due to HA but other macromolecules present in the protein fraction [30]. At this time, they were unable to isolate and characterize the proteins due to their small quantities and tendency to aggregate [30]. It wasn't until 1977, that Swann et al were able to isolate this lubricating glycoprotein from fractionation of bovine SF, naming it Lubricating Glycopeptide-I (LGP-I) [31].

In 1981, it was confirmed that LGP-I was responsible for the boundary lubricating properties of SF and could perform this function even in the absence of other constituents [32][33]. At this time LGP-I was renamed lubricin [32]. The MW of lubricin was determined by sedimentation-equilibrium measurements to be ~ 227.5 kDa [32][31] and 206 kDa by Rayleigh scattering [25], however it exhibits an apparent MW of 280 kDa with sodium-dodecyl sulfate polyacrylamide gel electrophoresis (SDS-PAGE) [25]. Schumacher et al. described a "novel" proteoglycan synthesized and secreted by chondrocytes in the superficial zone of articular cartilage [34]. This protein was named superficial zone protein (SZP) and exhibited an apparent MW of 345 kDa by SDS-PAGE [34]. Lubricin and SZP were classified as distinct SF constituents due to differences in cellular origin and migration on SDS-PAGE, but cDNA sequencing and homology analysis showed that both are products of the MSF gene, also known as the PRG4 gene [25]. Therefore, SZP and lubricin are collectively referred to as PRG4.

1.4.1 Structure – Function Relationship

The PRG4 gene consists of 12 exons and encodes for a 1404 amino acid protein, with a MW of ~ 150 kDa for the unmodified core proteins [25] . PRG4 has a central mucin-like domain that is extensively glycosylated with O-linked oligosaccharide substitutions and contains globular, cysteine-rich domains at the N- and C- termini (**Figure 1-5**) [25]. Approximately two thirds of the amino acid residues in the mucin domain are post-translationally modified with short O-linked glycans which gives this domain a strongly bound hydration layer that is responsible for PRG4's lubrication and antiadhesive properties [35]. The glycosylation on the mucin domain mainly consists of two glycans, -GalN-Gal and –GalN-GalN-Neu5Ac with a relative abundance of 33% and 66% respectively [35]. The –GalN-GalN-Neu5Ac glycan has a terminal sialic acid residue which carries an anionic charge, and as a result the mucin domain is negatively charged [35]. This

negative charge gives rise to repulsive hydration forces which contribution to boundary lubrication [36][37]. The end domains are hydrophobic and contain subdomains that display significant homology to the serum factor somatomedin B (SMB) at the N-terminus and plasma protein hemopexin (PEX) at the C-terminus, which are known to play a role in cell-cell and cell-ECM interactions such as binding [35][37]. These end domains are very "sticky" and can adhere to nearly all types of surfaces (hydrophobic, hydrophilic, anionic, cationic, etc), as well as interact with molecules such as collagen and HA [35]. Together, the adhesive end domains and non-adhesive central domain give rise to aggregation of PRG4 in solution with PRG4 dimers and possibly even trimers forming through adhesive coupling of end domains, and self-assembly behavior in which PRG4 adheres to surfaces through both end domains [35]. It has been shown that PRG4 forms inter- and intramolecular disulfide-bonded multimers in normal SF, and it is believed that these bonds are facilitated via the N- and C-termini of the protein [37][38]. Reduction and alkylation reduces the lubricating ability of PRG4 *in vitro*, as well as its ability to bind to the cartilage surface. This suggests that multimerization of PRG4 is a key structural component for its lubricating function [39].

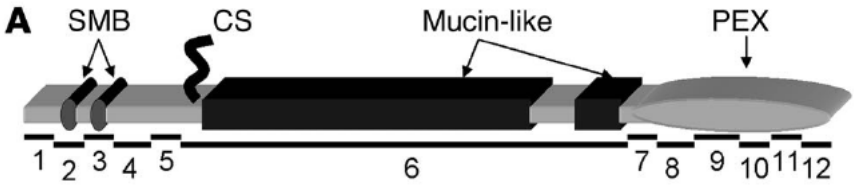

Figure 1-5. Schematic of a PRG4 monomer depicting the central mucin-like domain and the globular N- and C-termini. Adapted from [40].

PRG4 plays a key role in the reduction of friction between opposing cartilage surfaces, preventing degradation and adhesion of these surfaces. This function has been shown to be dependent on the O-linked oliogosaccharides in the central domains, possibly through the

generation of repulsive hydration forces or charge repulsion [39]. Deglycosylation of PRG4 results in a diminished lubricating ability and has been detected in different disease states [25]. This is consistent with the idea that PRG4 has glycosylation-dependent biophysical properties that have been observed in mucins [39]. PRG4's ability to interact with other SF constituents, specifically HA, also plays a key role in its ability to lubricate. It has been shown that though both PRG4 and HA alone significantly reduce friction compared to phosphate buffered saline (PBS), the coefficient of friction was lower when both PRG4 and HA were present [41].

In a healthy joint, a layer of PRG4 molecules covers the cartilage surface, acting as an antiadhesive and boundary lubricant, preventing cartilage damage [42]. Mutations to the PRG4 gene cause an autosomal recessive disorder called camptodactylyl-arthropathy-coxa vara-pericarditis (CACP) [43]. This disorder is characterized by pain, swelling, a restricted range of motion in large joints, and juvenile onset of non-inflammatory joint failure. The lack of functional PRG4 in CACP eventually leads to cartilage failure [25][42]. CACP in PRG4 knockout mice ($PRG4^{-/-}$) showed changes in cartilage including fibrillation at the cartilage surface and loss of superficial zone chondrocytes [42]. They also exhibited increased cartilage wear and higher friction in joints compared to wild-type animals ($PRG4^{+/+}$) [25]. Staining of coronal sections of knees showed a greater presence of active caspase-3, which is indicative of chondrocyte apoptosis, in $PRG4^{-/-}$ compared to heterozygous ($PRG4^{+/-}$) and wild-type mice [42]. The coefficient of friction in $PRG4^{-/-}$ was found to be more than double that of $PRG4^{+/+}$ [42]. An *in vitro* study with human SF and friction testing showed restoration of SF function when CACP SF was supplemented with PRG4 compared to CACP SF with no PRG4 added, as well as reduction in chondrocyte apoptosis [42]. This test also suggested that PRG4 acts synergistically with other SF components, such as HA, to lower kinetic friction since friction was lower in human SF compared to human PRG4

alone [42]. A reduction in PRG4 expression seen after joint injury is associated with cartilage degeneration, chondrocyte apoptosis, and onset of OA [25][42]. Therefore, PRG4 is imperative to the normal lubricating function of SF and maintenance of healthy joints.

The function of mucins and mucin-like proteins has been linked to their ability to form multimers via intermolecular disulfide bonds. A study by Schmidt et al. confirmed that PRG4 exists as a higher order disulfide-bonded dimer in normal SF [39][44]. Alvarez et al. found that this high MW multimer of PRG4 is synthesized and secreted by chondrocytes [44] in addition to forming naturally in SF. The ability of PRG4 to form multimers is facilitated by the N- and C-termini which form intra- and intermolecular disulfide bonds, and is critical to the various functions of mucins. The MW for PRG4 multimers has been reported to range from 867 to 1493 kDa [38]. Friction testing at a cartilage-cartilage interface showed that while both PRG4 containing the multimeric structure (PRG4Multi+) and PRG4 without the multimeric structure (PRG4Multi–) served as effective boundary lubricants, PRG4Multi+ was significantly more effective (**Figure 1-6**). It was also observed that the lubricating ability of PRG4Multi+ exhibits a concentration dependency, lubricating more effectively with higher concentrations over a range of 45 – 450 μg/mL. PRG4Multi– was not shown to be dose dependent [38]. In addition to superior lubrication, PRG4Mulit+ also demonstrated greater adsorption to the cartilage surface compared to PRG4Multi–. The adsorption to the cartilage surface of PRG4Multi+ was similar to that seen in normal SF. The reduction and alkylation of PRG4 has been previously shown to result in decreased binding to the cartilage surface and reduced lubricating ability at a cartilage-glass interface [38]. These findings suggest that the intermolecular disulfide bonds, and therefore the higher order multimeric structure of PRG4 play a key role in PRG4's lubricating ability.

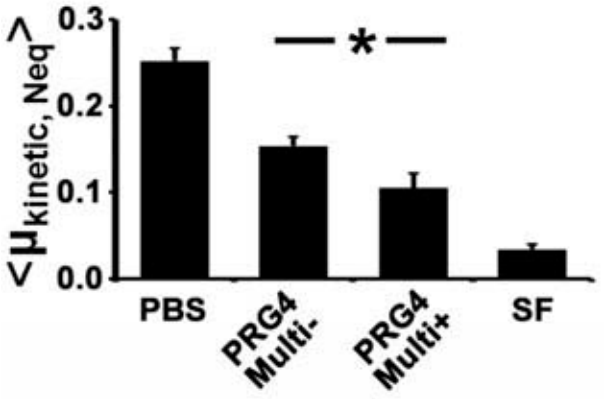

Figure 1-6. Kinetic $<\mu_{kinetic,\ Neq}>$ coefficient of friction of PRG4Multi– and PRG4Multi+ at 450 μg/mL. * indicates $p < 0.05$. Adapted from [38].

In addition to lubrication, PRG4 has other biophysical properties that allow it to contribute to joint health and maintenance. PRG4 is has both hydrophilic and hydrophobic domains allowing it to physisorb to a wide variety of surfaces. It is hypothesized that PRG4 adsorbs to hydrophobic surfaces via its hydrophobic N– and C – termini forming a loop-like conformation (**Figure 1-7a**) and adsorbs to hydrophilic surfaces via its central hydrophilic domain, forming a tail-like conformation (**Figure 1-7b**) [37]. It has been also suggested that PRG4 provides chondroprotective properties to SF by allowing strain energy induced through articular joint movement to slowly dissipate [25][39]. This appears to be due to PRG4 "entanglements" that are responsible for increasing the relaxation time of SF due to elastic contributions of PRG4 [25][39], as well as its interaction with HA [37].

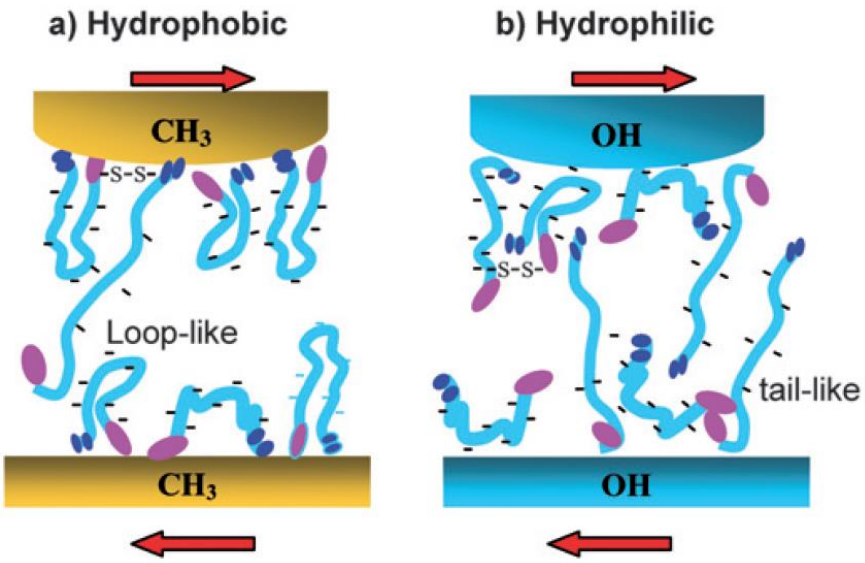

Figure 1-7. Schematic representation of adsorption of PRG4 on (**a**) hydrophobic and (**b**) hydrophilic surfaces. Adapted from [37]

1.4.2 PRG4 in Osteoarthritis

In OA, changes in SF PRG4 composition have been observed resulting in diminished cartilage boundary lubrication. Animal models have suggested a decrease in PRG4 concentration in secondary OA. Anterior cruciate ligament (ACL) injury in rabbits revealed an association between decreased PRG4 concentration and boundary lubricating ability, as well as increased cartilage degradation [10]. Recent studies also showed that local administration of PRG4 in ACL injury in animal models helps reduce the progression of OA and decrease cartilage degeneration. Lubricin synthesis was shown to be reduced in sheep, guinea pig and rat models of OA, suggesting that restoring PRG4 levels in OA joints could be beneficial as an OA therapy [45][46]. PRG4 concentration varies largely in OA human SF with observed concentration ranging from 276 – 762 ug/mL [47]. PRG4 in OA patients has been shown to be normal [47], diminished [10] and elevated [48] relative to normal SF PRG4 concentration.

A novel PRG4 construct, called LUB:1 was synthesized maintaining the native human PRG4 N– and C – termini domains, but had a shortened mucin domain [46]. Ex vivo functional assays showed that LUB:1 was able to efficiently bind and localize to articular cartilage surface, as is seen with full length PRG4 [46]. LUB:1 was also able to significantly improve cartilage boundary lubrication with maximal lubrication occurring at a similar concentration to that of full-length PRG4 [46]. Flannery et al., evaluated the therapeutic efficacy of LUB:1 by IA administration in a rat model of OA [46]. Rats that were treated with LUB:1 showed less cartilage lesions and degeneration than those that were administered PBS [46]. LUB:1 supplementation was also more effective in preventing cartilage degeneration during OA progression compared to PBS, and knee joints of rats treated with LUB:1 showed significantly less severe cartilage damage [46]. It has also been shown that treatment of acute ACL injury, which is a significant risk factor for OA, with PRG4 supplementation significantly reduced cartilage degeneration in rats [47]. A study by Ludwig et al. observed that OA SF deficient in PRG4 did not lubricate as well compared to normal SF and the friction coefficients observed were significantly higher [47]. With PRG4 supplementation the friction coefficients in PRG4 deficient OA SF were restored to normal, resulting in a significant decrease in friction [47]. Similar results were observed when PRG4 deficient OA SF was supplemented with PRG4 and HA [47]. This indicates that OA SF may result in a deficit of PRG4 which is associated with a diminished cartilage boundary lubricating ability. It also emphasizes that PRG4 is a critical boundary lubricant required for normal joint lubrication. Based on the results from these studies, PRG4 shows promise of being an effective biotherapeutic agent for the treatment of OA, as well as possibly improving the current treatment of HA viscosupplementation given their synergistic function.

1.4.3 Recombinant Human PRG4 (rhPRG4)

Recent technological advancements in protein expression have led to the expression of full-length recombinant human PRG4 (rhPRG4) using Chinese hamster ovary (CHO) cells [49][29]. rhPRG4 is expressed at high levels, > 1 g/L [50], which is necessary for clinical evaluation, and is available through Lμbris BioPharma (Framingham, MA, USA). Structurally, rhPRG4 has been shown to been able to form the higher order multimeric structure seen in PRG4, and also contains O-linked glycosylations. It has also been observed that rhPRG4 is able to adsorb to the cartilage surface and function as an effective boundary lubricant, as seen with native PRG4 [26]. Like native PRG4, rhPRG4 acts synergistically with HA to reduce friction at the cartilage surface [26]. Therefore, rhPRG4 has the potential to be used in humans as a form of OA therapy [51][52].

1.5 Supramolecular Chemistry

Supramolecular chemistry is the area of chemistry that focuses on chemical systems that are made up of a discrete number of assembled molecular subunits or components. The forces that are responsible for the spatial organization of the molecule can vary from weak forces, including intermolecular forces, electrostatic, or hydrogen bonding, to strong, such as covalent bonding. Where, traditional molecular chemistry focuses on atoms connecting together or breaking apart through covalent bonds, supramolecular chemistry studies the weaker and reversible non-covalent interactions between molecules [53]. The forces studied include hydrogen bonding, hydrophobic interactions, electrostatic effects, and cation-π interactions which have a vital role in the building of supramolecular structures.

1.5.1 Hydrogen Bonding

Hydrogen bonds are usually stronger than van der Waals interactions, but weaker than ion – ion interactions with bond energies varying from 0.2 – 40 kcal/mol [54]. These bonds are formed

between an electronegative atom on one molecule (hydrogen bond acceptor) and a hydrogen atom bonded to an electronegative atom on another molecule (hydrogen bond donor). The hydrogen atom is bonded directly to the electronegative atom, such as oxygen or nitrogen, and begins to develop a significant positive charge, attracting the lone electron pair on the electronegative atom. This type of bonding can occur both inter- and intramolecularly [53].

1.5.2 Hydrophobic Interactions

Hydrophobic interactions describe the relationship between water and lipophilic groups. Lipophilic molecules are nonpolar and do not interact with water, therefore forming intermolecular aggregates in water and other polar media. These interactions are driven by the tendency of the polar water molecules to interact with the polar part of the lipophilic molecule, forming a stable hydrogen bonded network [53]. These types of interactions are important in the folding and recognition of biomolecules, and in the formation of host – guest complexes [53].

1.5.3 Electrostatic Interactions

Electrostatic interactions usually arise from Coulombic forces between charged molecules, such as those present in ion-ion interactions [53]. These interactions include polarization interactions that arise from dipole moments between ions and molecules, and therefore include both ion-ion and ion-dipole interactions. Electrostatic interactions can be either attractive or repulsive depending on the types of charges that are interacting with each other. These types of interactions contribute to both the stabilizing and destabilizing of supramolecular complexes [53].

1.5.4 Cation – π Interactions

Cation-π interactions occur between an electron rich π systems and an adjacent cation. Aromatic rings have a partial negative charge due to delocalized π electrons attracting cationic moieties. These interactions contain an electrostatic component, require specific geometries to

occur and can be fairly strong [55][56]. In proteins, a cation-π interaction can occur between cationic sidechains of either arginine or lysine and aromatic sidechains of phenylalanine, tyrosine or tryptophan [55].

Supramolecular chemistry has demonstrated many important concepts including but not limited to molecular self-assembly, molecular recognition, and host-guest chemistry [57]. The study of these non-covalent interactions is very important in understanding many biological processes, which often rely on these types of forces for structure and function. Therefore, biological systems are often the driving force of supramolecular research.

1.6 Calcium Interactions with Proteins

Calcium is a divalent ion that is known to form calcium-ion-bridging interactions. These interactions are a type of physical cross-link formed when a calcium ion forms coincident ionic bonds with two anions located on adjacent negatively charged macromolecules or within different regions on a single macromolecule [35]. Calcium has previously been shown to affect the structure and organization of mucins. MUC5B mucin, the predominant oligomeric mucin in saliva, showed a major decrease in the diffusion of microspheres in the presence of $CaCl_2$ [58]. The apparent pore size in saliva decreased from ~ 1200 to 300 nm after the addition of $CaCl_2$, suggesting that calcium had a major effect on the organization of MUC5B in saliva [58]. Exposure to $CaCl_2$ also resulted in the formation of a high MW macromolecular fraction with a 6-fold increase in average MW [58]. Calcium has been shown to have a particular affinity for carboxylate groups and inducing aggregation behavior in glycoproteins via this binding [35]. Carboxylates on sialic acid residues account for a vast majority of the negative charge in PRG4, providing a potential binding site for calcium ions.

A study by Greene et al. to evaluate PRG4 layer surface morphology, mechanical properties, and adhesion forces in $CaCl_2$ revealed structural changes induced by calcium ion interactions that significantly altered key properties [35]. PRG4 was deposited on a silicon wafer and exposed to 20 mM of $CaCl_2$ resulting in significant changes in PRG4 layers compared to PRG4 in PBS [35]. These measurements showed three distinct layers of PRG4 in $CaCl_2$ when deposited onto the silicon wafer compared to one in PBS, suggesting a structural rearrangement produced by the formation of calcium ion-bridging interactions [35]. Changes in the adhesion properties of PRG4 were also observed upon exposure to $CaCl_2$ [35]. PRG4 exposed to calcium ions bound more tightly to a silica surface and exhibited a larger adhesion energy [35]. However, whether this is calcium-ion bridging interactions or simply an enhanced PRG4-silica interaction remains unclear [35].

1.7 Arginine Interactions with Proteins

Arginine is a useful solvent additive in the biotechnology and pharmaceutical industries for many applications, including suppression of protein aggregation and non-specific adsorption during formulation and purification [59][60][61] by suppressing protein-protein and protein-surface interactions [62]. There are implications however that arginine may be a protein-denaturant, possibly limiting the expansion of its applications. The idea that arginine is a protein-denaturant arises because arginine decreases melting temperature and alters the spectroscopic properties of some proteins. Arginine also contains a guanidinium group, which is critical to the denaturing activity of guanidine hydrochloride further implicating its ability be involved in protein denaturation [59]. While it's been shown that arginine is not in fact a protein-denaturant like guanidine hydrochloride it does affect the properties of some proteins. Measurements of the protein activity of *Halobacetrium salinus* nucleoside disphosphate kinase (HsNDK) showed a

decrease in protein activity to 70 and 36 % in the presence of 1 and 2 M arginine respectively [59]. This suggests that arginine may affect substrate binding or catalytic activity. It is believed that arginine is able to suppress protein aggregation by binding to folding intermediates but only at the surface thereby preventing aggregation, but not protein denaturation. Another possible mechanism by which arginine inhibits protein aggregation is through its ability to form dimers. It has been shown that arginine is able to form dimers through hydrogen bonding of the carboxylate and N-terminal of adjacent arginine molecules [61]. It was observed that the formation of hydrogen bonds increased with an increase in arginine concentration as arginine dimers can interact with other arginine dimers or free arginine molecules [61]. This increases the size of arginine resulting in accumulation at the protein surface which prevents protein-protein interaction. Arginine has also been found to interact with the protein surfaces via its guanidinium group and interacts strongly with aromatic and charged residues on the protein surface via hydrogen bonding [61]. This crowding effect of arginine is enhanced by its ability to self-associate, which along with its ability to interact with protein residues via its guanidinium group appear to be the main mechanism by which arginine prevents aggregation [61]. Using hydrophobic interaction chromatography (HIC), it has been shown that arginine weakens hydrophobic interactions of proteins [60]. This was demonstrated by the elution of two monoclonal antibodies, IgG4-A and IgG4-B from a phenyl-Sepharose column [60]. In the absence of arginine only 16% of IgG4-A eluted and 60% of IgG4-B. When 0.5 M arginine was added to the ammonium sulfate elution buffer this weakened the hydrophobic interactions of the antibodies with the column and recovery rose to 45% for IgG4-A and ~ 85% for IgG4-B [60]. It was also shown using ion exchange chromatography (IEC) that addition of arginine to a protein sample of interleukin-6 (IL-6) led to a ~ 40% reduction in protein aggregation [60].

1.8 PRG4 Interaction with Calcium and Arginine

Calcium and arginine have been shown to be present in SF at ~ 5 mM [35] and ~ 45 – 95 μM [63] respectively. Despite the importance of PRG4 in joint lubrication and health there have been few studies investigating the potential interactions between PRG4 and calcium or arginine and their potential effects on the structure and properties of PRG4. Though calcium has been shown to have an affinity for negatively charged carboxylate groups [35] and induce structural and properties changes in PRG4 self-assembled layers and other mucins [35][58], its effects on the supramolecular structure of rhPRG4 remain to be fully elucidated. Arginine is known to interact with charged residues such as those seen on the sialic acid residues of PRG4, but the interaction between arginine and PRG4 is unknown. Since arginine has the ability to disrupt protein aggregation it may affect the ability of PRG4 to assemble into a higher order structure and could interfere with PRG4 lubrication, though these effects remain to be elucidated. It has been shown previously that exposure to guanidine diminished PRG4, purified from bovine cartilage explant culture, lubricating ability and altered its structure [64], however it is unknown if arginine demonstrates the same effect. The availability of highly purified rhPRG4 now makes it possible to study the potential interactions of calcium and arginine with rhPRG4, whereas in the past only highly enriched PRG4 from purified bovine SF and/or cartilage explant culture has been available.

1.9 Hypothesis and Aims

Both calcium and arginine have been shown to be important mediators in protein-protein aggregation, and could therefore be critical in formulation development of a therapeutic rhPRG4 preparation. Given the evidence for a PRG4 structure-function observed with PRG4 disulfide bonded structure and cartilage boundary lubricating function, it is possible (rh)PRG4

supramolecular structure can mediate lubricating function as well. Though rhPRG4 has the negatively charged sialic residues that are important in binding of arginine and calcium the interaction of rhPRG4 with these molecules and their effect on rhPRG4 supramolecular structure formation and lubricating ability have yet to be determined. *Therefore, the hypothesis of this thesis is that PRG4 exists in a non-covalent supramolecular structural form that is necessary for its boundary lubricating properties. This hypothesis will be tested by the following aims:*

Aim 1: Characterization of the supramolecular structure of PRG4, and its dependency on concentration

Aim 2: Elucidation of the types of molecular forces underlying the formation of the supramolecular structure

Aim 3: Determination of the lubricating function of PRG4 preparations enriched and devoid of the supramolecular structure

Chapter 2: Methods

2.1 rhPRG4 Sample Preparation

Highly purified human recombinant PRG4 (rhPRG4) was obtained from Lμbris BioPharma (Framingham, MA) [29], derived from Chinese hamster ovary (CHO) cells as described previously [29][49]. Briefly, the gene encoding the full length 1404 amino acid human PRG4 was inserted into plasmid vectors, commercially available at Selexis SA (Switzerland), then the CHO cells were cultured in stirred bioreactors, and subsequently the protein was purified via depth filtration, a 4-step chromatographic purification process followed by subjected to ultrafiltration/diafiltration into PBS resulting in a stock rhPRG4 at 1.24 – 2.4 mg/mL. Samples were diluted to test concentrations of 50, 150, 450, and 1200 μg/mL (from Batch 1712) with PBS, or to a test concentration of 450 μg/mL in PBS, arginine (0.2 M) (Sigma-Aldrich, St. Louis, MO, USA), and calcium (20 mM) (Sigma-Aldrich, St. Louis, MO, USA) (from Batch 1608). PBS was filtered through a 0.1 μm Millipore filter prior to addition of the rhPRG4 solution. rhPRG4 solutions were shaken and allowed to incubate overnight at 4 °C prior to testing.

2.2 Gel Electrophoresis and Western Blotting

2.2.1 Background

Electrophoresis is a widely used technique for separating and isolating proteins, based on their ability to move through a conductive medium in response to an applied electric field [65]. The electrophoretic mobility of a protein depends on factors such as size, charge, and shape. Typically, electrophoresis is performed on a polyacrylamide gel immersed in conducting buffer. Proteins migrate as anions toward the cathode, with the gel acting as a size select sieve, and smaller proteins moving more quickly and further down the gel than larger ones. In polyacrylamide gel electrophoresis (PAGE), proteins are usually separated in the presence of a detergent and under

denaturing conditions. The most commonly used detergent is sodium dodecyl sulfate (SDS), which acts to shield the charge of proteins in the mixture, providing them all with a negative charge [66]. This allows for separation based on molecular weight. Gel electrophoresis can also be done in the absence of SDS, maintaining the native structure of the protein by Native PAGE. In the absence of SDS, the proteins are separated based on their charge to mass ratio rather than molecular weight, with the mobility of the protein largely depending on hydrodynamic size and negative charge density [66]. Once protein separation is complete, the gel can be further processed for Western Blotting, which allows for the detection of specific proteins using target specific antibodies. Western blotting with PRG4 has been done previously using monoclonal antibody 9G3 [26] and LPN [29] [67].

2.2.2 Analysis

2.2.2.1 SDS-PAGE

Various preparations of rhPRG4 were characterized by sodium dodecyl sulfate polyacrylamide gel electrophoresis (SDS-PAGE) and Western blot as described previously [25] [39]. All materials and reagents were obtained from Thermo Fisher Scientific (Carlsbad, CA, USA) unless otherwise stated. rhPRG4 samples were mixed with NuPAGE® LDS Sample Buffer and heated for 10 minutes at 70°C. The samples were then loaded onto a Novex 3 – 8 % Tris-Acetate gel, along with 10 μL of HiMark® Pre-Stained High Molecular Weight (HMW) Protein Standard. Electrophoresis was done in NuPAGE® Tris-Acetate SDS Running Buffer at 150 V for 75 minutes at 4°C in a vertical gel apparatus. The gels were then electroblotted in NuPAGE® Transfer Buffer onto 0.2 μm PVDF blotting membranes at 200 mA for 2 hours at 4 °C. Membranes were blocked with 5 % non-fat dry milk in Tris-buffered saline with 0.1 % (v/v) Tween 20 (TBST: 20 mM Tris-base, 137 mM NaCl, pH = 7.6) for 1 hour at room temperature. The membranes were

rocked overnight at 4°C in the following primary antibody solutions in 3% non-fat dry milk in TBST: mAb 9G3 (0.4 μg/mL) (Millipore Sigma, Temecula, CA, USA). Membranes were washed in TBST (3 x 10 minutes), and rocked for 1 hour at room temperature in the following secondary antibody solution in 3% non-fat dry milk: goat anti-mouse IgG HRP (0.0126 μg/mL) (Sigma-Aldrich, St. Louis, MO, USA). Membranes were washed in TBST (3 x 10 minutes) and developed using ECL Prime. Immunoreactive bands were visualized using Amersham™ Imager 600 (GE Healthcare Bio-Science AB, Uppsala, Sweden).

2.2.2.2 Native PAGE

Native PAGE and western blotting were used to characterize the apparent molecular weight (MW) of immunoreactive rhPRG4 as described by the manufacturer's proctocol (Thermo Fisher Scientific, Carlsbad, CA, USA). All materials and reagents used were obtained from Thermo Fisher Scientific (Carlsbad, CA, USA) unless otherwise noted. Samples were mixed with NativePAGE™ Sample Buffer and loaded onto a NativePAGE™ Novex® 3 – 12 % Bis-Tris gel, along with 10 μL of NativeMark™ Unstained Protein Standard. Electrophoresis was done in NativePAGE™ Cathode Buffer (10 mL NativePAGE™ Running Buffer 190 mL deionized water) at 150 V for 60 minutes, followed by 250 V for 30 minutes at 4°C in a vertical gel apparatus. The gel was then electroblotted in NuPAGE® Transfer Buffer onto 0.2 μm PVDF blotting membranes at 200 mA for 2 hours at 4 °C. Membranes were blocked with 5 % non-fat dry milk in Tris-buffered saline with 0.1 % (v/v) Tween 20 (TBST: 20 mM Tris-base, 137 mM NaCl, pH = 7.6) for 1 hour at room temperature. The membranes were rocked overnight at 4°C in the following primary antibody solutions in 3% non-fat dry milk in TBST: mAb 9G3 (0.4 μg/mL) (recognizes and binds to the mucin domain) and mAb LPN (0.2 μg/mL) (recognizes and binds to the C-terminal). Membranes were washed in TBST (3 x 10 minutes), and rocked for 1 hour at room temperature in

the following secondary antibody solutions in 3% non-fat dry milk: goat anti-mouse IgG HRP for mAb 9G3 (0.0126 μg/mL), and goat anti-rabbit IgG HRP (Millipore Sigma, Temecula, CA, USA) for Ab LPN. Membranes were washed in TBST (3 x 10 minutes) and developed using ECL Prime. Immunoreactive bands were visualized using Amersham^{TM} Imager 600.

2.3 Dynamic Light Scattering

2.3.1 Background

Photon correlation spectroscopy (PCS), also known as dynamic light scattering (DLS), is a widely used technique for the characterization of particle size across the range of 0.3 nm – 10 μm. This technique has also been used to characterize the aggregation behavior of molecules dispersed in a liquid [7][69]. DLS is a non-destructive analytical technique that can be used to measure the size distribution of particles suspended in solution. In a DLS measurement, a laser beam is passed through the solution measuring the speed of particles undergoing Brownian motion, which is the random motion of particles resulting from collisions with the solvent molecules surrounding them [70]. When light hits a particle, it is scattered due to a process called Rayleigh scattering, where the intensity of light scattered fluctuates over time. These time-dependent fluctuations in the scattering intensity can then be used to obtain diffusion coefficient and particle size information [70][71]. The diffusion coefficient can be converted to particle size using the Stokes-Einstein equation:

$$d_H = \frac{kT}{3\pi\eta D}$$

where d_H is the hydrodynamic diameter, k is Boltzmann's constant, T is absolute temperature, η is dispersant viscosity, and D is diffusion coefficient [72]. DLS results are expressed as hydrodynamic diameter, which relates the size of particles being measured to that of a hypothetical sphere with the same diffusion coefficient in the same viscous environment [70]. DLS size

measurements are displayed as an intensity size distribution in which the scattered intensity is proportional to the diameter of the particles to the sixth power [68]. This distribution is weighted in respect to larger particles and aggregates, thus over representing them. This can be advantageous for sensitive detection of small quantities of aggregates but provides a disadvantage when measuring smaller particles in the presence of larger aggregates. The intensity based distribution data can be transformed to volume and number distributions using Mie theory, which describes the scattered intensity as a function of the particle size [68]. The volume distribution is also weighted towards large particles and aggregates with the volume of a sphere proportional to the particle diameter to the third power. Conversely, the number distribution is directly proportional to particle size. Mie theory makes the following three assumptions to make the transformation from intensity to volume and number distributions: (1) all particles are spherical, (2) all particles have a homogenous and equivalent density, (3) the optical properties of the particle being measured are known. Though the assumptions of Mie theory may introduce limitations to the validity of the conversion [73], the number distribution is useful for the detection of smaller particles that may be under represented in the intensity and volume distributions. Mean particle size, can also be determined from DLS, and is often expressed in terms of Z-average. The Z-average is an intensity-weighted mean hydrodynamic diameter, making it sensitive to the presence of large aggregates [70]. This value is typically used for monodisperse samples, however has been shown to be valid for bimodal distributions [73].

2.3.2 Analysis

Size distribution measurements were performed using DLS on a Malvern Zetasizer Nano ZS (Malvern Instruments, Worcestershire, UK), equipped with a solid-state 532 nm He/Ne laser at a scattering angle of 173°C. Samples were measured in disposable polystyrene cuvettes at a

temperature of 25 ± 0.1 °C under the conditions that the refractive index of rhPRG4 is 1.457 with an absorption of 0.220, and the refractive index of PBS is 1.33, with a viscosity (η) of 0.8882 cP, and dielectric constant of 79. Arginine buffer was prepared in PBS and measurements done under the conditions stated previously. Calcium buffer was prepared in Tris-base (20 mM) in water and measurements done under the conditions that the refractive index of water is 1.33, η is 1 cP, and dielectric constant is 80.4. Size distribution measurements were done in triplicate (n = 3), calculated using Dispersion Technology Software version 5.03 (Malvern Instruments), and averaged over N = 3 trials.

2.3.3 Statistical Analysis

To access the effect of rhPRG4 concentration and the effect of buffer on rhPRG4 size, the Z-average measurements were obtained for each sample. Data is expressed as the mean ± standard error of the mean (SEM). Statistical analysis was implemented using SPSS Statistics 24.0 (IBM; Armonk, NY). One-way analysis of variance (ANOVA) with LSD post-hoc testing was implemented to test for statistical significance ($p < 0.05$).

2.4 Friction Testing

2.4.1 PDMS-Glass Tribology Tests

2.4.1.1 Background

Tribology is the study of wear, friction and lubrication between two sliding surfaces [74]. Friction is the resistance to motion, whose magnitude is a function of the materials, geometries and surface features of the bodies in contact with one another [74]. It is usually desirable to minimize friction in order to maximize the efficiency of a component or process [74]. In general, friction increases with both load and surface roughness, and can be decreased by using a lubricant. When tribology occurs in the human body or in animals it is known as biotribology, integrating

tribology with biology and medicine [75]. The study of friction within synovial joints is classified as biotribology [75]. There is a broad range of test setups that can be used for the determination of friction coefficients for lubricants. In the joint, cartilage is loaded via an oscillatory movement with a migrating contact, which can be best simulated by a linearly reciprocating tribometer [21]. This test set-up is compatible with a variety of test interfaces such as polydimethylsiloxane (PDMS)-glass, latex-glass, and cartilage-glass, and allows for classic Stribeck analysis at different lubricating regimes [21][76]. Stribeck analysis has been used to test the lubrication modes of synthetic interfaces against each other, and a synthetic material against cartilage [14][76][77]. However, these results may not be comparable to that of cartilage-cartilage due to its soft and porous interface, as well as the ability of putative lubricants to interact with a physiological articulating surface [23] .

The tribology unit that supports the sample uses a lateral spring system, which ensures that the applied normal force is evenly distributed onto each of the three cylindrical samples, minimizing lateral shear (**Figure 2-1**) [21]. An applied normal force of 6 N has been shown to allow for the probing of the boundary lubrication regime and ensures full and even contact between the sphere and cylinder samples [21][76]. Though the use of a synthetic material interface may not allow for all physiological molecular interactions to occur, PRG4 has been shown to demonstrate low friction properties at both synthetic [13][78] and physiological [24] interfaces [79].

Figure 2-1. Schematic illustration of tribological set-up of three cylindrical samples with a spherical probe. Adapted from [21].

2.4.1.2 Tribology Tests

The tribology measurements were performed using a ball-on-cylinder geometry on a MCR 302 rate-controlled rotational rheometer equipped with a tribology unit (Anton Paar, Graz, Austria) as described previously [76]. Measurements were done at a controlled temperature of 37 ± 0.1°C and a normal tribological force of 6.0 ± 0.1 N, at a PDMS-glass interface, with a borosilicate glass ball and 6 mm PDMS plugs. PDMS was made by combining silicone elastomer base and curing agent (Sylgard 184 Silicone Elastomer, Dow Corning Corporation, Midland, MI, USA) at a 10:1 mass ratio. This mixture was centrifuged at 300 rpm for five minute to eliminate air bubbles before pouring into a petri dish. The PDMS was then left to cure overnight at room temperature. The test sequence consisted of a 5-minute incubation, followed by pre-conditioning, where the spinning velocity of the ball was increased from 0 to 1000 mm/s. Once a velocity of 1000 mm/s was reached, 26 measurements were recorded as the velocity was decreased to 0.01 mm/s. All tribological measurements were conducted in duplicate (n = 2), and averaged over N = 3 trials.

2.4.1.3 Tribology Test Sequences

One test sequence was implement to access the effect of rhPRG4 concentration on rhPRG4 lubricating ability at a PDMS-glass interface.

(1) Lubricating Ability of rhPRG4 at Four Concentrations Compared to PBS Alone. The effect of rhPRG4 lubricating ability at four concentrations was assessed via the following test sequence:

Test Sequence 1 (n=3): PBS, PBS+rhPRG4(50 μg/mL), PBS+rhPRG4(150 μg/mL), PBS+rhPRG4(450 μg/mL), PBS+rhPRG4(1200 μg/mL)

Three additional test sequences were used to assess the effect of buffer on the lubricating ability of rhPRG4 at a PDMS-glass interface. For each test sequence two concentrations of rhPRG4 were used (150 and 450 μg/mL).

(2) Lubricating Ability of rhPRG4+PBS compared to PBS Alone. The effect of PBS on rhPRG4 lubricating ability was assessed via the following test sequence:

Test Sequence 2 (n = 3): PBS, PBS+rhPRG4(150 μg/mL), PBS+rhPRG4(450 μg/mL)

(3) Lubricating Ability of rhPRG4+Arginine compared to Arginine Alone. The effect of arginine buffer (0.2 M) on rhPRG4 lubricating ability was assessed via the following test sequence:

Test Sequence 3 (n = 3): Arginine, Arginine+rhPRG4(150 μg/mL), Arginine+rhPRG4(450 μg/mL)

(4) Lubricating Ability of rhPRG4+Calcium compared to Calcium Alone. The effect of calcium buffer (20 mM) on rhPRG4 lubricating ability was assessed via the following test sequence:

Test Sequence 3 (n = 3): Calcium, Calcium+rhPRG4(150 μg/mL), Calcium+rhPRG4(450 μg/mL)

2.4.1.4 Statistical Analysis

To access the boundary lubricating ability of each test lubricant, the kinetic coefficient of friction ($\mu_{kinetic}$) was measured as described in Section 2.4.1.2. Data is expressed as the mean ± SEM. Statistical analysis was implemented using SPSS Statistics 24.0 (IBM; Armonk, NY).

Test Sequence 1: $\mu_{kinetic}$ changed only slightly with values at a velocity of 0.01 mm/s being on average within 14.5 ± 1.2 % of those at a velocity of 1000 mm/s. Therefore, for clarity, statistical analysis of $\mu_{kinetic}$ data was implemented for a velocity of 0.398 mm/s only. Two-way ANOVA with Tukey post-hoc testing was used to assess the effect of concentration on rhPRG4 lubricating ability.

Test Sequence 2, 3, and 4: $\mu_{kinetic}$ changed greatly between 0.01 mm/s and 1000 mm/s. Therefore, statistical analysis was implemented for velocities of 0.398 and 3.98 mm/s. Two-way ANOVA with repeated measures and LSD post-hoc testing was used to assess the effect of buffer on rhPRG4 lubricating ability.

ANOVA is robust to heterogeneity of variances as long as the number of tests within each group is equal or nearly equal [80]. This test is also robust to the assumption of normality, with the validity of the test being only slightly affected by considerable deviations from normality [80].

2.4.2 Cartilage Boundary Lubrication Tests

2.4.2.1 Background

In vitro test setups using synthetic materials may not allow for all physiologically relevant interactions of surfaces and their putative lubricants. Therefore, *in vitro* mechanical tests can also be done at a physiological interface, such as cartilage-cartilage. Articular cartilage acts as the low

friction, wear resistant, load bearing tissue at the end of long bone in skeletal joints [16][41]. During movement, such as walking, the articulation of cartilage against cartilage, presents a major biomechanical challenge, often resulting in deterioration of the cartilage with age and disease [41]. However, when healthy, articular cartilage provides low friction and low wear properties to the synovial joint through a combination of lubrication mechanisms [24][41]. Typically, the modes of lubrication in synovial joints can be classified as either fluid film or boundary lubrication, depending on a variety of factors [24]. The friction coefficient, μ, which is defined as the ratio of tangential friction force to the normal force, provides a quantitative measure [24]. An assortment of time-dependent *in vitro* mechanical tests have been developed to assess both the effectiveness and modes of lubrication of articular cartilage. Since joints are subject to alternating periods of rest and motion, the transition from rest to motion, as well as steady-state motion present challenges with lubrication [24]. Friction coefficients can be measured at start-up from a static condition (μ_{static}) or under steady sliding, kinetic conditions ($\mu_{kinetic}$). Cartilage-on-cartilage lubrication tests use a configuration that mimics certain aspects of naturally articulating surfaces, and can be done in either a sliding or rotational configuration, where the contact areas are either moving or constant, respectively [24]. Though, the sliding test configuration models physiological kinematics, the rotational configuration is advantageous for examining boundary lubricants of articular cartilage at a like interface [24]. In the sliding configuration, both fluid film and boundary lubrication are in effect due to fluid pressurization and exudation, even at slow sliding velocities [24]. In the rotational configuration, ploughing friction losses are minimized since the apposed surfaces remain in contact and fluid pressure effects are minimal at slow velocities after the initial pressure dissipates [24]. This configuration also reduces variations in sliding velocity and the time required for fluid depressurization [24].

2.4.2.2 Sample Preparation

Stock solutions of purified rhPRG4 were diluted to test a concentration of 450 μg/mL in PBS, arginine (0.2 M), and calcium (20 mM). Bovine SF was obtained from Animal Technologies Inc. (Tyler, TX, USA).

Osteochondral samples were prepared, as described previously [24][41], from the patellofemoral groove of four bovine stifle joints obtained from a local abattoir (Calgary, AB). Osteochondral blocks were isolated, and osteochondral samples (n = 12) were cut from the blocks using a low speed drill press with custom stainless steel coring bits and PBS at room temperature for irrigation. Each sample pair consisted of a core (radius = 6 mm), and annulus (outer radius, R_o = 3.2 mm and inner radius, R_i = 1.5 mm), both with central holes (radius = 0.5 mm) drilled into and exiting the bone to facilitate fluid depressurization. Samples were then rinsed and shaken vigorously overnight in PBS at 4 °C to remove any residual SF from the articular cartilage. The cartilage thickness of each core and annulus was measured using digital calipers at four equally spaced locations around the circumference and averaged. Samples were then bathed in subsequent test lubricants, completely immersing the cartilage, at 4 °C overnight prior to testing.

2.4.2.3 Lubrication Tests

The lubricating ability of each of the rhPRG4 test solutions was assessed using a Bose ELF 3200 (Bose ElectroForce Systems Group, Eden Prairie, MN) using a previously characterized in vitro cartilage-cartilage boundary mode friction test (**Figure 2-2**) [24]. Samples were secured concentrically with the annulus above and the core below. A lubricant bath was formed by securing an inert silicone rubber tube around the core and adding test lubricant, completely immersing both cartilage surfaces. The samples were then compressed to 18% of the total cartilage thickness at a constant rate of 0.002 mm/s, followed by a 40-minute stress relaxation to enable depressurization

of the interstitial fluid. The samples were then rotated +/- 2 revolutions at an effective velocity of 0.3 mm/s, which has been shown to maintain boundary mode lubrication at a depressurized articular cartilage-cartilage surface [24], with pre-sliding durations (Tps; duration the sample is stationary prior to rotation, also known as dwell time) of 1200, 120, 12 and 1.2 seconds. The test sequence was then repeated in the opposite direction of rotation, -/+ 2 revolutions.

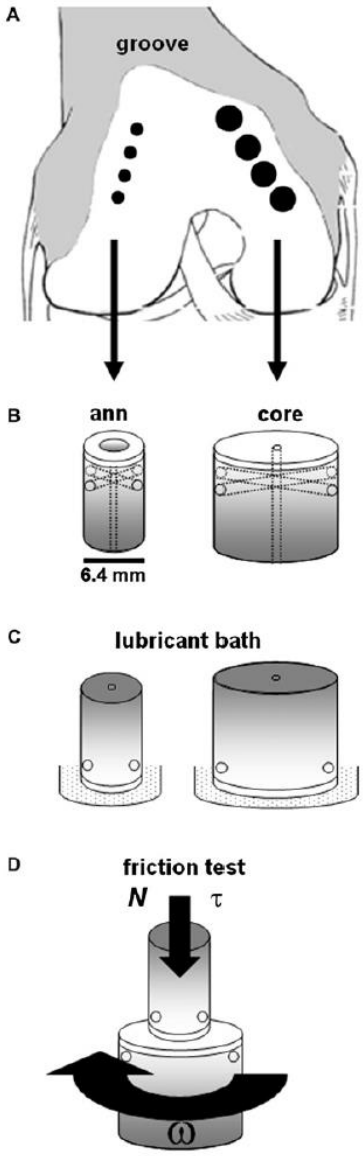

Figure 2-2. Schematic illustration of in vitro cartilage-cartilage boundary lubrication test. Osteochondral blocks were harvested from the patellofemoral groove of bovine stifle joints (**A**) and annulus (ann) and core samples were prepared (**B**). Samples were incubated at 4 °C for 24 hr in test lubricant (**C**) prior to testing (**D**). Adapted from [24]**.**

2.4.2.4 Lubrication Test Sequences

Three test sequences were used to assess the effect of buffer on the lubricating ability of rhPRG4, at 450 μg/mL, at a cartilage-cartilage interface. In each test sequence, PBS served as the negative control, and bovine SF as the positive control.

(1) Cartilage Boundary Lubricating Ability of rhPRG4+PBS Compared to PBS Alone. The effect of PBS on rhPRG4 lubricating ability was assessed via the following test sequence:

Test Sequence 1 (N = 4): PBS, PBS, rhPRG4+PBS, SF

(2) Cartilage Boundary Lubricating Ability of rhPRG4+Arginine Compared to Arginine Alone. The effect of arginine on rhPRG4 lubricating ability was assessed via the following test sequence:

Test Sequence 2 (N = 4): PBS, Arginine, Arginine+rhPRG4, SF

(3) Cartilage Boundary Lubricating Ability of rhPRG4+Calcium Compared to Calcium Alone. The effect of calcium on rhPRG4 lubricating ability was assessed via the following test sequence:

Test Sequence 3 (N = 4): PBS, Calcium, Calcium+rhPRG4, SF

2.4.3 Statistical Analysis

2.4.3.1 Cartilage-Cartilage Friction Testing

To access the boundary lubricating ability of each test lubricant, two coefficients of friction, static ($\mu_{static,Neq}$) and kinetic ($<\mu_{kinetic,Neq}>$) were measured as described previously [24] and averaged between + and - revolutions. Data is expressed as the mean ± SEM. Statistical analysis was implemented using SPSS Statistics 24.0 (IBM; Armonk, NY). For test sequences 1, 2, and 3, $<\mu_{kinetic,Neq}>$ values at Tps = 1.2 were within 34.5 ± 1.8 %, 31.0 ± 1.1 %, and 31.2 ± 1.7 %

respectively compared to Tps = 1200. Therefore, $<\mu_{kinetic,Neq}>$ data is presented for Tps = 1.2s only for clariy. The effect of buffer solution on rhPRG4 lubricating ability at a cartilage-cartilage interface was assessed using a two way repeated measures ANOVA with LSD post-hoc testing.

Chapter 3: Results

3.1 Effect of Concentration on rhPRG4 Size and Lubricating Ability at a PDMS-Glass Interface

3.1.1 Western Blotting

Native PAGE and SDS PAGE western blotting indicated the presence of mAb 9G3 immunoreactive species in each of the rhPRG4 preparations as well as the presence of a higher order structure. Native PAGE western blotting (**Figure 3-1A**) showed a distinct high molecular weight (MW) band (**) at the top of the gel, as well as a lower MW species (*) migrating with an apparent MW of ~1236 kDa. SDS PAGE western blotting (**Figure 3-1B**) also showed a distinct band slightly above 460 kDa (*), and the higher MW species near the top of the gel (**).

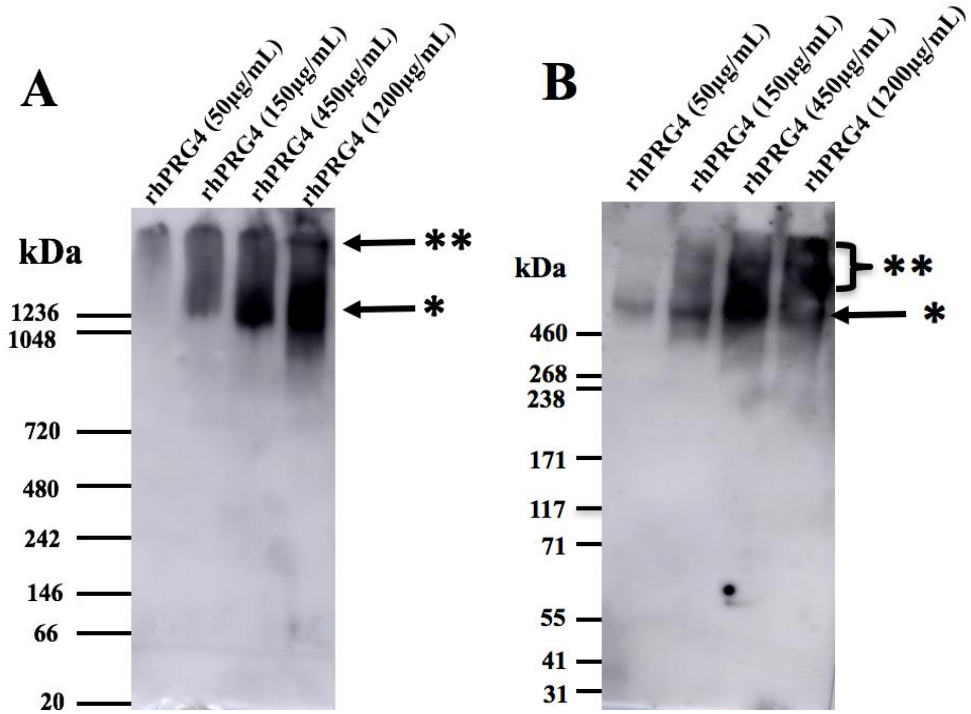

Figure 3-1. Native PAGE (**A**) and SDS-PAGE (**B**) western blot of rhPRG4 at concentrations of 50, 150, 450, and 1200 µg/mL with mAb 9G3.

3.1.2 Dynamic Light Scattering

The major peaks in the number (**Figure 3-2A**) for rhPRG4 at concentrations of 50, 150, 450, and 1200 μg/mL exhibited a concentration dependency, indicating an increase in size with concentration. There were two major peaks in the number distribution of rhPRG4 (50 μg/mL) at ~ 23.5 (4.2%) and ~ 44.9 (5.5%). Four major peaks were observed in rhPRG4 (150 μg/mL) at ~ 19.5 (4.3%), ~ 27.0 (4.5%), ~ 35.6 (2.5%), and ~ 71.0 (2.2%). Three major peaks were observed in rhPRG4 (450 μg/mL) at ~ 29.6 (3.6%), ~ 37.0 (4.5%), and ~ 68.0 (3.0%). In rhPRG4 (1200 μg/mL) three major peaks were observed at ~ 27 (3.7), ~ 32.5 (4.1%), and ~ 74.6 (3.4%).

The intensity distribution (**Figure 3-2B**) showed similar results, suggesting a concentration dependency with rhPRG4 size, increasing with concentration. Two major peaks were observed in rhPRG4 (50 μg/mL) at ~ 49.2 (0.5%) and ~ 216 (2.7%). One major peak was observed in rhPRG4 (150 μg/mL) at ~ 197 (3.3%). Two major peaks were observed in rhPRG4 (450 μg/mL) at ~ 42.9 (0.5%) and ~ 206 (3.8%). One major peak was observed in rhPRG4 (1200 μg/mL) ~ 248 (3.1%).

The Z-average provides an intensity weighted mean hydrodynamic radius, that is very sensitive to the presence of protein aggregates. This allows for a direct, clear comparison of particle size between different samples. The Z-average indicated an increase in average particle size with an increase in rhPRG4 concentration (**Figure 3-2C**). The Z-average was largest for rhPRG4 (1200 μg/mL) at 181.90 ± 0.027 nm and smallest for rhPRG4 (50 μg/mL) at 158.90 ± 0.019 nm. rhPRG4 (150 μg/mL) and rhPRG4 (450 μg/mL) were intermediate at 164.31 ± 0.013 and 167.00 ± 0.046 nm respectively.

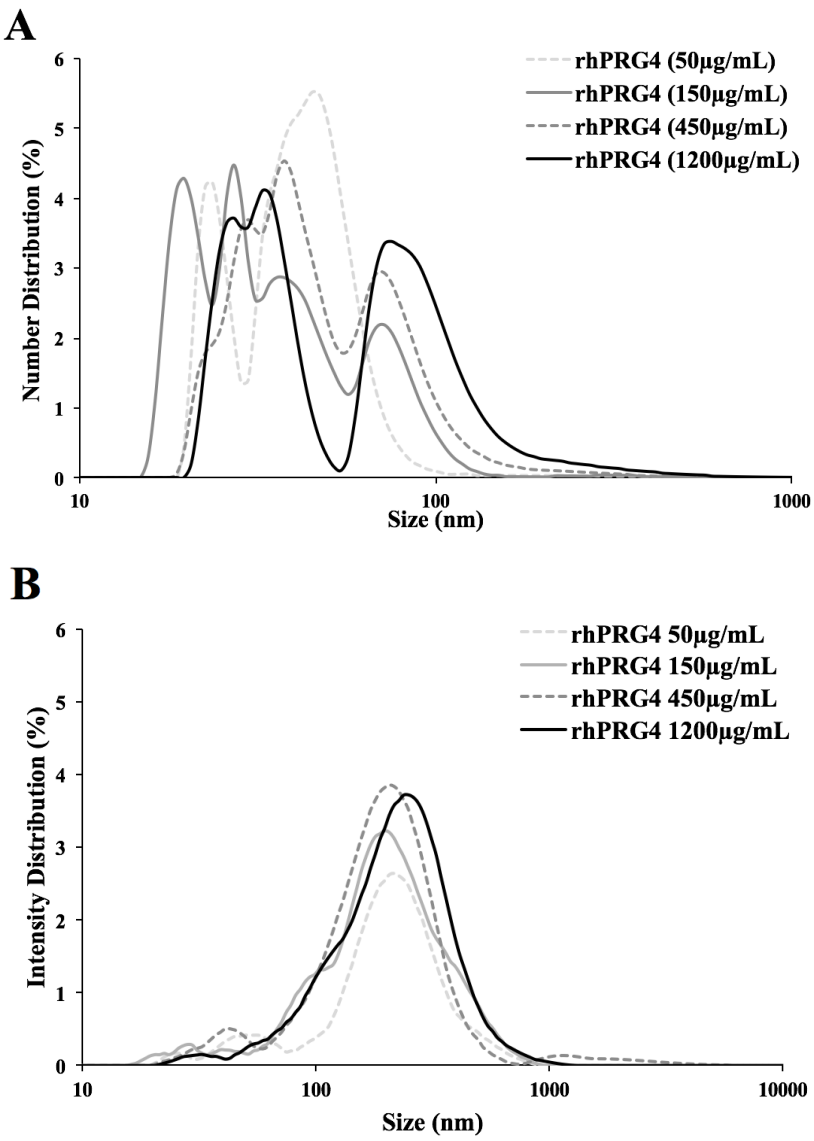
A
rhPRG4 (50µg/mL)
rhPRG4 (150µg/mL)
rhPRG4 (450µg/mL)
rhPRG4 (1200µg/mL)
Number Distribution (%)
Size (nm)
B
rhPRG4 50µg/mL
rhPRG4 150µg/mL
rhPRG4 450µg/mL
rhPRG4 1200µg/mL
Intensity Distribution (%)
Size (nm)

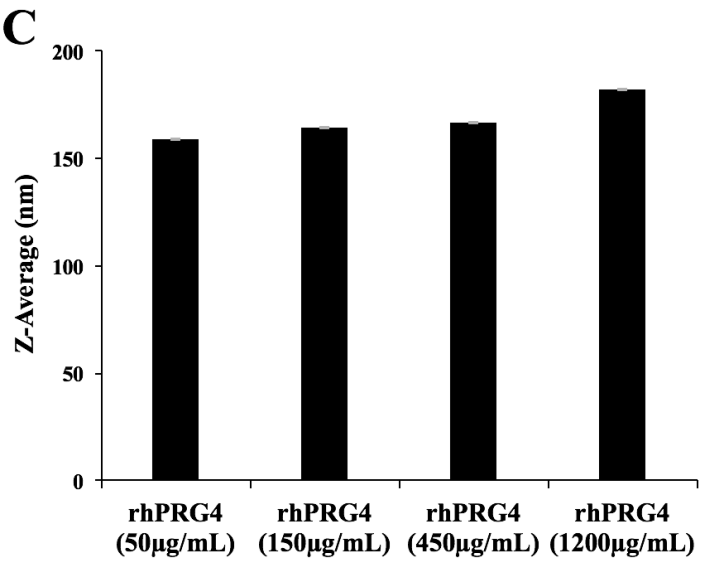

Figure 3-2. Number distribution (%) (**A**) and intensity distribution (%) (**B**) versus particle size (hydrodynamic diameter, nm) of rhPRG4 at concentrations of 50, 150, 450, 1200 μg/mL (N = 3) and Z-average (**C**) demonstrating the mean ± SEM size of particles in solution increasing with concentration.

3.1.3 Tribology Measurements

rhPRG4 functioned as an effective boundary lubricant at a PDMS-glass interface in a dose-dependent manner, with $\mu_{kinetic}$ decreasing with increased rhPRG4 concentration. $\mu_{kinetic}$ varied with velocity ($p > 0.05$) and test lubricant ($p < 0.05$) with no interaction ($p = 1$) (**Figure 3-3A**). Values were consistently highest in PBS and lowest with a rhPRG4 concentration of 1200 μg/mL. rhPRG4 concentrations of 50, 150, 450 μg/mL were intermediate. $\mu_{kinetic}$ for PBS was significantly higher compared to rhPRG4 50 μg/mL ($p = 0.002$), 150 μg/mL ($p = 0$), 450 μg/mL ($p = 0$), and 1200 μg/mL ($p = 0$) μg/mL at a velocity of 0.398 mm/s (**Figure 3-3B**). This velocity was chosen because it occurs in boundary lubrication mode and is similar to the velocity of 0.3 mm/s used in friction testing at a cartilage-cartilage interface.

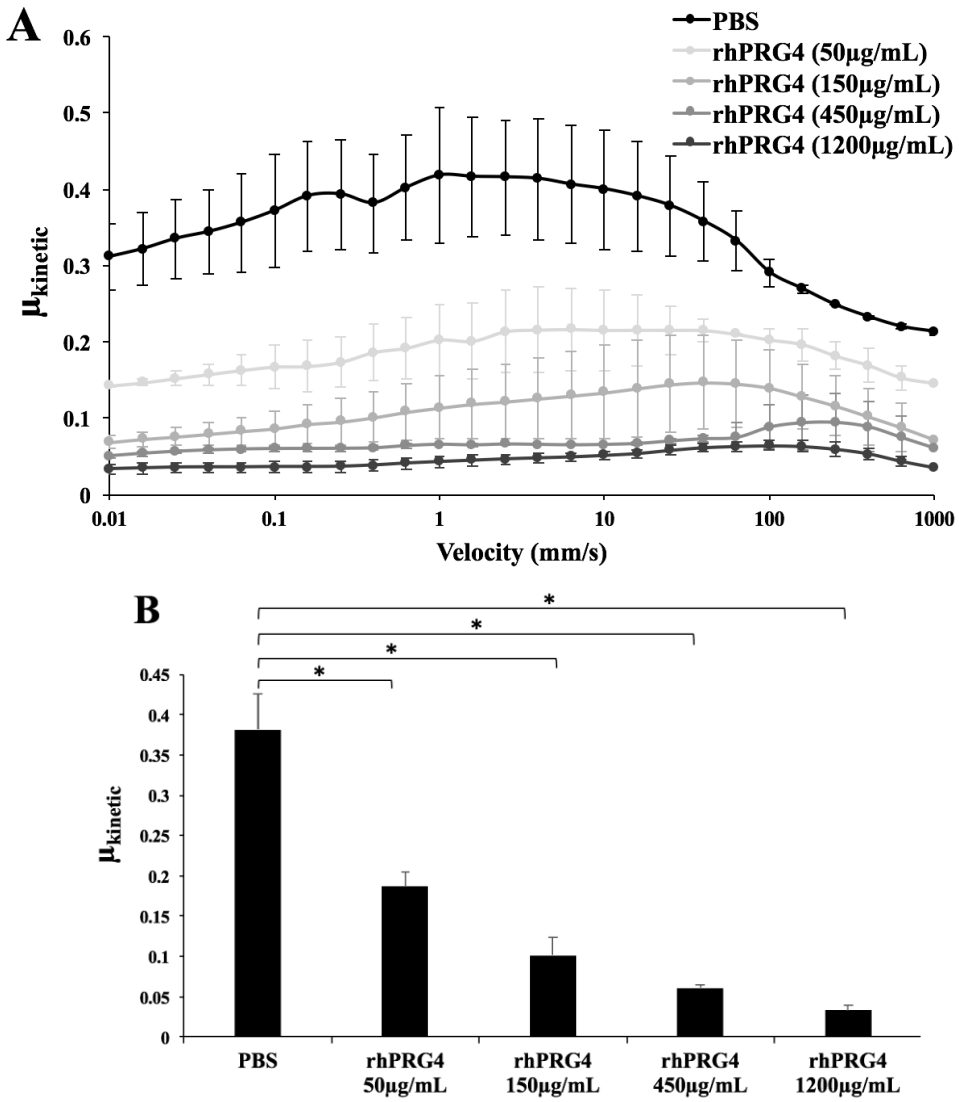

Figure 3-3. Stribeck curve of $\mu_{kinetic}$ of rhPRG4 at concentration of 50, 150, 450, and 1200 μg/mL at velocities of 0.01 – 1000 mm/s, showing a decrease in $\mu_{kinetic}$ with increasing rhPRG4 concentration (**A**) (N = 3). $\mu_{kinetic}$ was significantly decreased with increasing rhPRG4 concentration compared to PBS at a velocity of 0.398 mm/s (**B**). * denotes $p < 0.05$.

At a PDMS-glass interface the addition of rhPRG4 at concentrations of 50, 150, 450, and 1200 μg/mL was able to reduce the coefficient of friction of PBS across all velocities. This reduction in friction was statistically significant at 0.398 mm/s. The coefficient of friction also

decreased with increasing rhPRG4 concentration with rhPRG4 at 50 μg/mL resulting in the highest friction values and rhPRG4 at 1200 μg/mL providing the lowest friction values. The coefficient of friction between varying rhPRG4 concentrations demonstrated a decreasing trend towards lower values.

3.2 Effect of Buffer on rhPRG4 Size/Structure and Lubricating Ability at a PDMS-Glass Interface

3.2.1 Western Blotting

Western blotting showed each of the rhPRG4 preparations in PBS, arginine (0.2 M), and calcium (20 mM) contained both mAb 9G3 (**Figure 3-4A**) and Ab LPN (**Figure 3-4B**) immunoreactive species. 9G3 recognizes the central mucin domain and LPN recognizes the C-terminal. 9G3 showed a band (*) with an apparent MW of ~ 1048 kDa in rhPRG4 preparations in PBS, arginine, and calcium, which was strongest in PBS. rhPRG4 in calcium demonstrated more enriched immunoreactivity in a high MW species (**) near the top of the gel. This high MW species was also present in PBS and arginine preparations though to a lesser extent. The LPN blot showed a distinct high MW immunoreactive band near the top of the gel. rhPRG4 prepared in calcium was enriched in this high MW species (**) compared to PBS and arginine. A second band of a lower MW species (*) migrating with an apparent MW of ~ 1236 kDa in PBS and calcium preparations, but is absent in arginine.

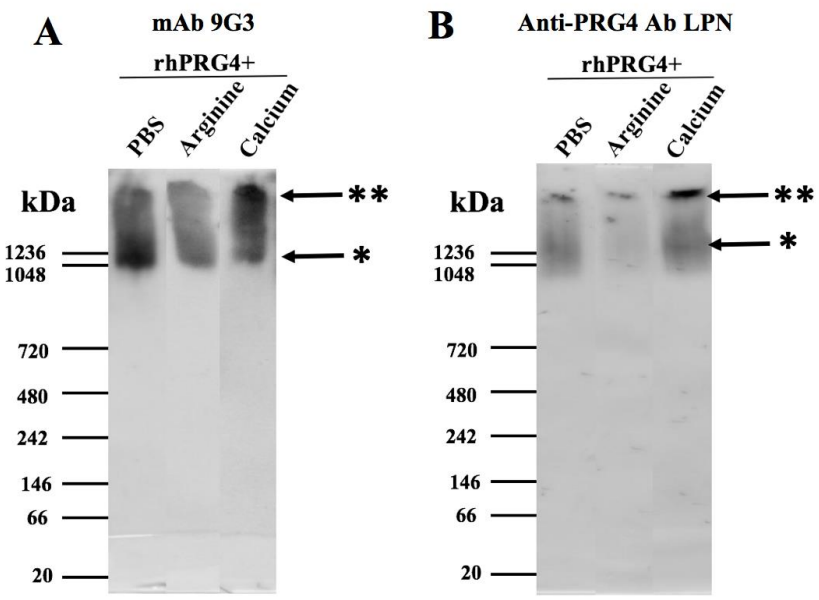

Figure 3-4. Western blot of rhPRG4 (450 μg/mL) in PBS, Arginine (0.2 M), and Calcium (20 mM) with mAb 9G3 (**A**) and Anti-PRG4 Ab LPN (**B**).

3.2.2 Dynamic Light Scattering

The major peaks in the number distributions for rhPRG4 in calcium were greater than in PBS and arginine indicating the presence of a larger molecular structure (**Figure 3-5A**). The major peaks in the distributions for rhPRG4 in arginine were less than in both calcium and arginine. There were four major peaks in the number distribution of calcium at ~ 11 (3%), ~ 24 (7%), ~ 68 (5%), and ~ 458 (3%) nm. One major peak was observed for each PBS and arginine at ~ 28 (24%) and ~ 24 (23%) nm respectively. This is similar to what was observed previously with PBS+rhPRG4(450 μg/mL), however the previous sample exhibited a higher presence of dimers.

The intensity distribution showed similar results, indicating an increase in particle size for rhPRG4 in calcium, and a decrease in size for rhPRG4 in arginine, compared to rhPRG4 in PBS (**Figure 3-5B**). The intensity distribution of calcium showed three major peaks at ~ 32.0 (0.8%), ~ 190 (1.8%) and ~ 712 (14%) nm. The intensity distribution of PBS showed two major peaks at

~ 32.7 (1.6%) and ~ 220 (12%) nm, which is similar to what was observed previously. Two major peaks were observed for arginine at ~ 37.8 (2.6%) and ~ 220 (11%) nm.

The intensity-weighted Z-average indicated an increase in average particles size when rhPRG4 was in calcium compared to in PBS or arginine. It also showed a decrease in average particle size when rhPRG4 was in arginine compared to PBS or calcium. The average particle size of rhPRG4 was significantly larger in calcium at 664.02 ± 56.9 nm compared to 164.02 ± 3.8 and 147.5 ± 3.9 nm in PBS and arginine respectively (**Figure 3-5C**) (p = 0).

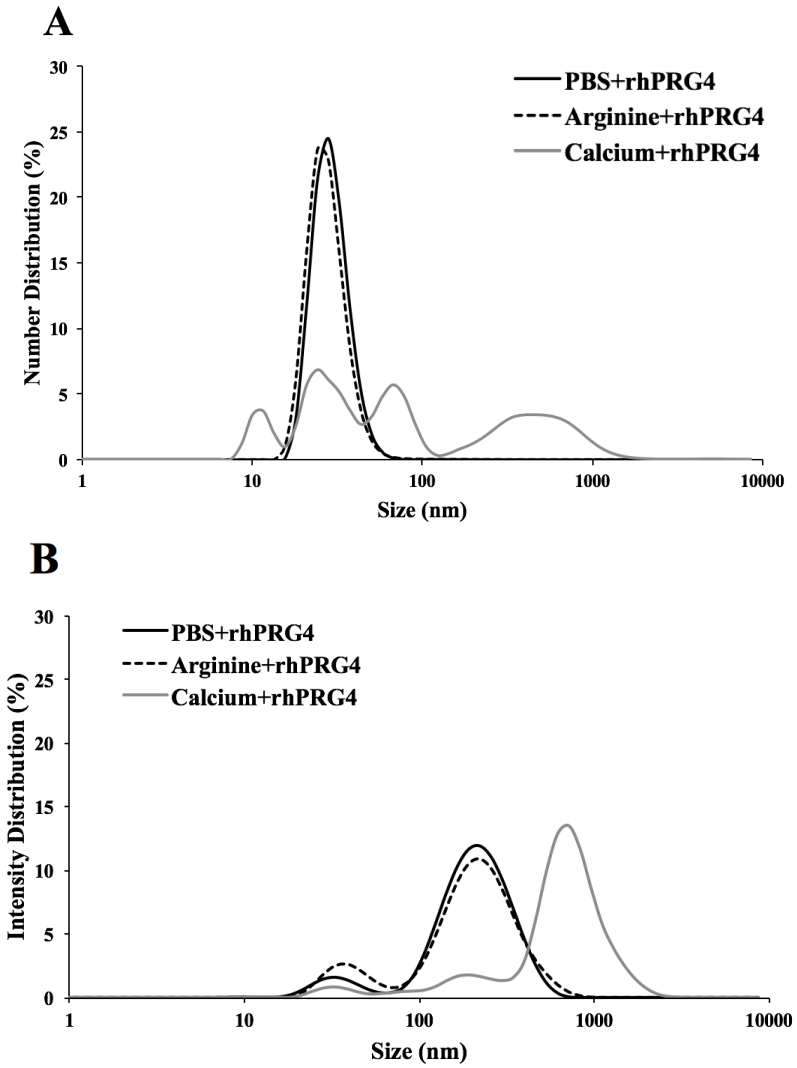

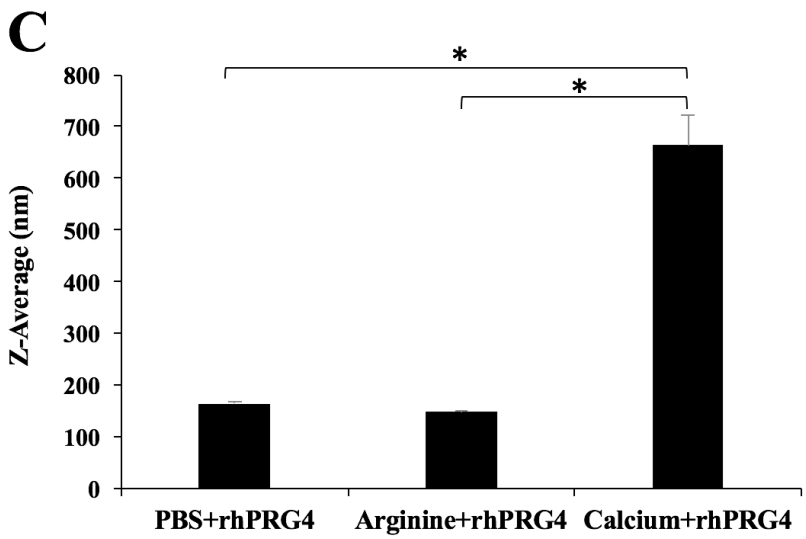

Figure 3-5. Number distribution (%) (**A**) and intensity distribution (%) (**B**) versus particle size (hydrodynamic diameter, nm) of rhPRG4 (450 μg/mL) in PBS, Arginine (0.2 M), and calcium (20 mM) (N = 3). The Z-average showing the average hydrodynamic size of particles in solution was significantly different in Calcium+rhPRG4 compared to PBS+rhPRG4 and Arginine+rhPRG4 (**C**). * denotes $p < 0.05$.

3.2.3 Tribology Measurements

3.2.3.1 Lubricating Ability of PBS+rhPRG4 at a PDMS-Glass Interface Compared to PBS Alone

PBS demonstrated higher coefficient of friction values across all velocities compared to rhPRG4. rhPRG4 in PBS functioned as an effective boundary lubricant at 0.398 mm/s and 3.98 mm/s. These velocities were chosen because both are slow enough to represent boundary lubrication and 0.398 mm/s is similar to the velocity of 0.3 mm/s used in friction testing at a cartilage-cartilage interface. $\mu_{kinetic}$ varied with both velocity ($p > 0.05$) and lubricant ($p < 0.05$) with no interaction ($p = 0.810$) (**Figure 3-6A**). Values were consistently higher in PBS compared to PBS+rhPRG4, while PBS+rhPRG4(150 μg/mL) and PBS+rhPRG4(450 μg/mL) were similar.

At a velocity of 0.398 mm/s PBS was significantly higher than PBS+rhPRG4(150 μg/mL) ($p = 0.011$) and PBS+rhPRG4(450 μg/mL) ($p = 0.009$). $\mu_{kinetic}$ was also significantly higher in PBS compared to PBS+rhPRG4(150 μg/mL) ($p = 0.012$) and PBS+rhPRG4(450 μg/mL) ($p = 0.011$) at 3.98 mm/s (**Figure 3-6B**). PBS+rhPRG4(150 μg/mL) and PBS+rhPRG4(450 μg/mL) were not different at 0.398 mm/s ($p = 0.681$) or 3.98 mm/s ($p = 0.350$).

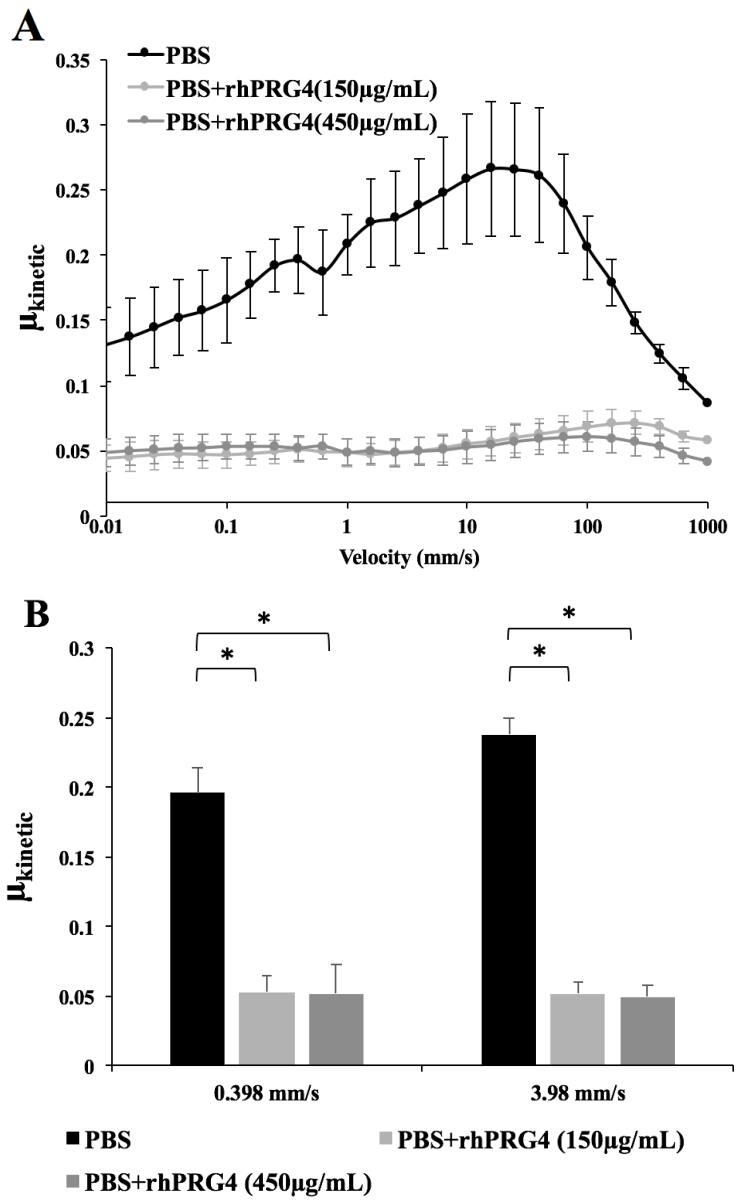

Figure 3-6. Stribeck curve showing $\mu_{kinetic}$ of PBS, PBS+rhPRG4(150 µg/mL), and PBS+rhPRG4(450 µg/mL) at velocities of 0.01 – 1000 mm/s (**A**) (N = 3). $\mu_{kinetic}$ was significantly decreased upon addition of rhPRG4 compared to PBS at velocities of 0.398 and 3.98 mm/s (**B**). * denotes $p < 0.05$.

3.2.3.2 Lubricating Ability of Arginine+rhPRG4 at a PDMS-Glass Interface Compared to Arginine Alone

rhPRG4 did not improve the lubricating ability of arginine (0.2 M) at various velocities at a PDMS-Glass interface. $\mu_{kinetic}$ varied with both velocity ($p < 0.05$) and lubricant ($p > 0.05$) with no interaction ($p = 0.375$) (**Figure 3-7A**). Below 63.096 mm/s values were consistently lowest in arginine, and highest in arginine+rhPRG4(450 μg/mL), while arginine+rhPRG4(150 μg/mL) was intermediate. Above 63.096 mm/s $\mu_{kinetic}$ was highest in arginine and lowest in arginine+rhPRG4(450 μg/mL), while arginine+rhPRG4(150 μg/mL) was intermediate. There was no difference between lubricants (**Figure 3-7B**).

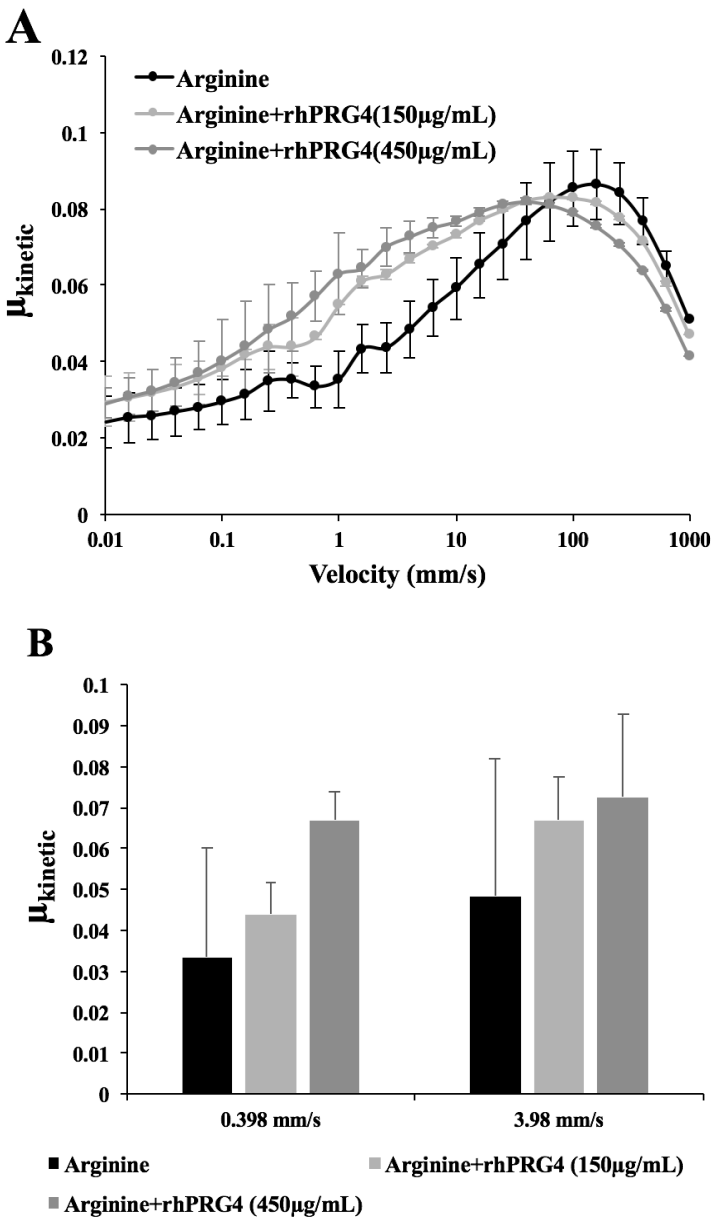

Figure 3-7. Stribeck curve of $\mu_{kinetic}$ of Arginine, Arginine+rhPRG4(150 μg/mL), and Arginine+rhPRG4(450 μg/mL) at velocities of 0.01 – 1000 mm/s (**A**) (N = 3). $\mu_{kinetic}$ increased upon addition of rhPRG4 compared to Arginine at velocities of 0.398 and 3.98 and mm/s (**B**).

3.2.3.3 Lubricating Ability of Calcium+rhPRG4 at a PDMS-Glass Interface Compared to Calcium Alone

rhPRG4 in calcium (20 mM) functioned as an effective friction reducing boundary lubricant at a PDMS-glass interface across all velocities. $\mu_{kinetic}$ varied with both velocity ($p > 0.05$) and lubricant ($p < 0.05$) with an interaction ($p = 0.013$). Values were consistently highest in calcium and lowest in calcium+rhPRG4 (450 μg/mL), while calcium+rhPRG4(150 μg/mL) was intermediate (**Figure 3-8A**). $\mu_{kinetic}$ was significantly higher in calcium compared to calcium+rhPRG4 (150 μg/mL) and calcium+rhPRG4(450 μg/mL) at velocities of 0.398 ($p = 0.005$ and 0.014 respectively) and 3.98 ($p = 0.008$ and 0.007 respectively) mm/s (**Figure 3-8B**). calcium+rhPRG4(150 μg/mL) and calcium+rhPRG4(150 μg/mL) were not different from each other at a velocity of 0.398 mm/s ($p = 0.959$) or 3.98 mm/s ($p = 0.380$).

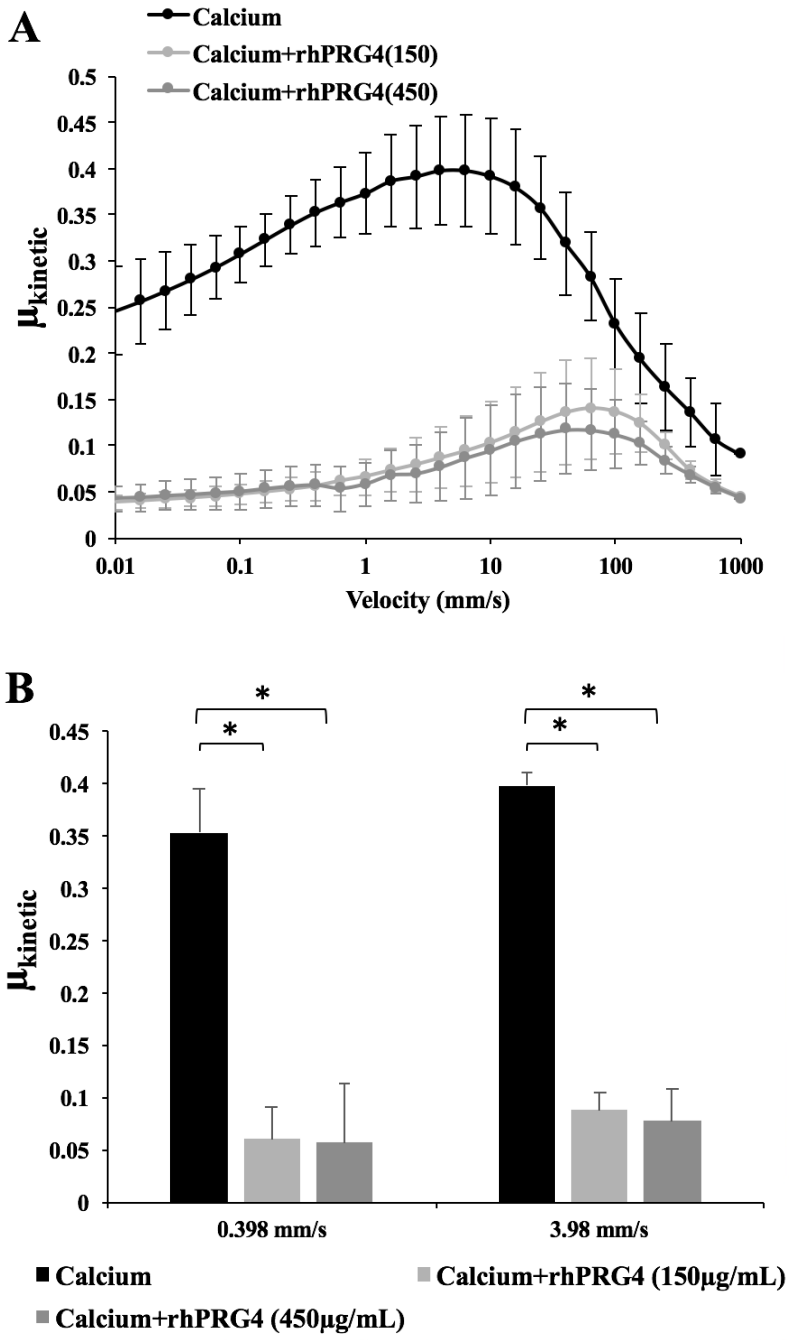

Figure 3-8. Stribeck curve showing $\mu_{kinetic}$ of Calcium, Calcium+rhPRG4(150 μg/mL), and Calcium+rhPRG4(450 μg/mL) at velocities of 0.01 – 1000 mm/s (**A**) (N = 3). $\mu_{kinetic}$ was significantly decreased upon addition of rhPRG4 to Calcium compared to Calcium alone at velocities of 0.398 and 3.98 mm/s (**B**). * denotes $p < 0.05$

At a PDMS-glass interface rhPRG4 was able to reduce the coefficient of friction of PBS across all velocities between 0.01 and 1000 mm/s. This reduction in friction showed a trend to lower friction values at velocities of 0.398 and 3.98 mm/s. The addition of rhPRG4 to arginine (0.2 M) reduced friction above 63.096 mm/s, but increased friction below 63.096 mm/s. The increase in friction at 0.398 and 3.98 mm/s showed a trend of increasing friction values with increasing rhPRG4 concentration. rhPRG4 reduced the coefficient of friction of calcium (20 mM) across all velocities between 0.01 and 1000 mm/s. This decrease in friction was statistically significant at 0.398 and 3.98 mm/s. These findings suggest that the ability of rhPRG4 to form its supramolecular structure is important for its function as a boundary lubricant.

3.3 Effect of Buffer on Lubricating Ability of rhPRG4 at a Cartilage-Cartilage Interface

3.3.1 Cartilage Boundary Lubricating Ability of PBS+rhPRG4 Compared to PBS Alone

PBS+rhPRG4 functioned as an effective friction reducing cartilage boundary lubricant at a concentration of 450 μg/mL compared to PBS alone. $\mu_{static,Neq}$ varied both with Tps and test lubricant ($p < 0.05$) with an interaction ($p = 0$). Values increased with Tps and were highest in PBS and lowest in SF, while PBS+rhPRG4 was intermediate (**Figure 3-9A**).

$<\mu_{kinetic,Neq}>$ values showed a similar trend, varying with test lubricant and Tps ($p < 0.05$), increasing only slightly with Tps, with an interaction ($p = 0.035$). Values at Tps = 1.2 s were greatest in PBS (0.104 ± 0.042) and lowest in SF (0.024 ± 0.006), with PBS+rhPRG4 (0.052 ± 0.010) in between (**Figure 3-9B**). $<\mu_{kinetic,Neq}>$ was significantly higher in PBS+rhPRG4 compared to SF at Tps = 1.2 s ($p = 0.027$).

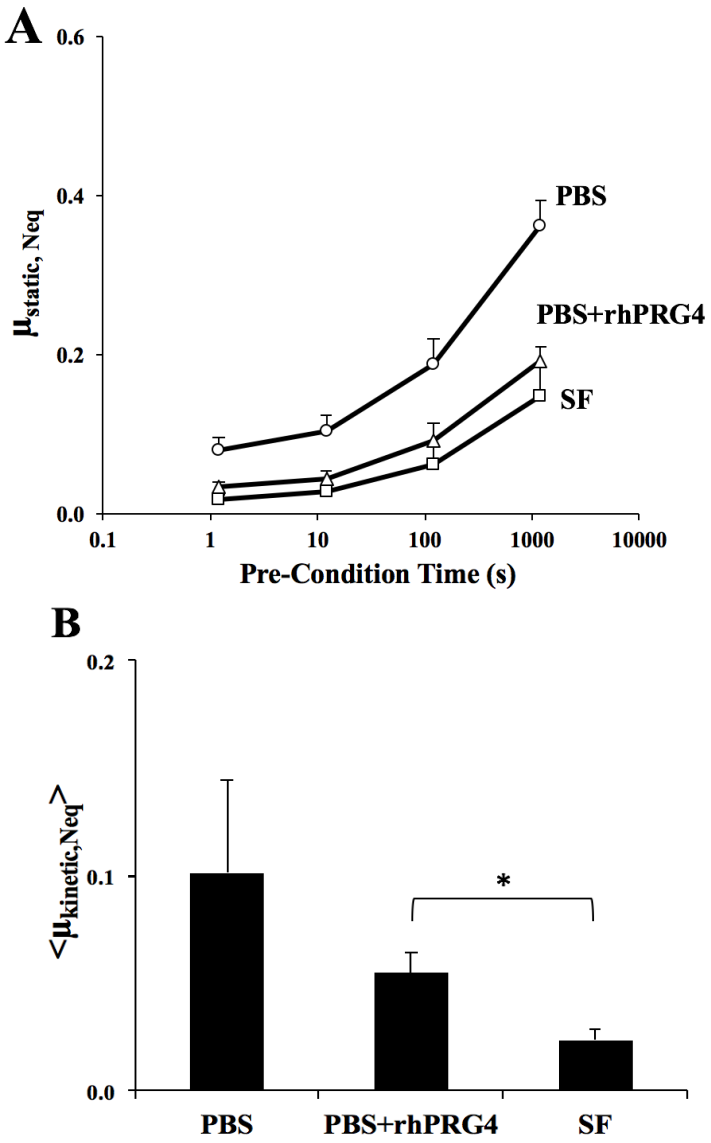

Figure 3-9. Static ($\mu_{static,Neq}$) (**A**) and kinetic ($<\mu_{kinetic,Neq}>$) at Tps = 1.2 s (**B**) friction coefficients of PBS, PBS+rhPRG4 and SF with rhPRG4 preparations at 450 μg/mL (N = 4). * denotes $p < 0.05$.

3.3.2 Cartilage Boundary Lubricating Ability of Arginine+rhPRG4 Compared to Arginine Alone

Addition of rhPRG4 (450 μg/mL) to arginine (0.2 M) did not improve the lubricating ability of arginine. $\mu_{static,Neq}$ varied with Tps and test lubricant ($p < 0.05$) with an interaction ($p =$

0). Values increased with Tps and were consistently highest for Arginine+rhPRG4 and lowest in SF, while arginine was intermediate (**Figure 3-10A**).

$<\mu_{kinetic,Neq}>$ values showed similar trends, varying with Tps and test lubricant ($p < 0.05$) , increasing only slightly with Tps, with no interaction ($p = 0.232$). At Tps = 1.2 s $<\mu_{kinetic,Neq}>$ was greatest in Arginine+rhPRG4 (0.061 ± 0.011), lowest in SF (0.025 ± 0.004), and intermediate for Arginine (0.041 ± 0.006)) (**Figure 3-10B**). Values for Arginine+rhPRG4 were significantly higher than SF ($p = 0.029$).

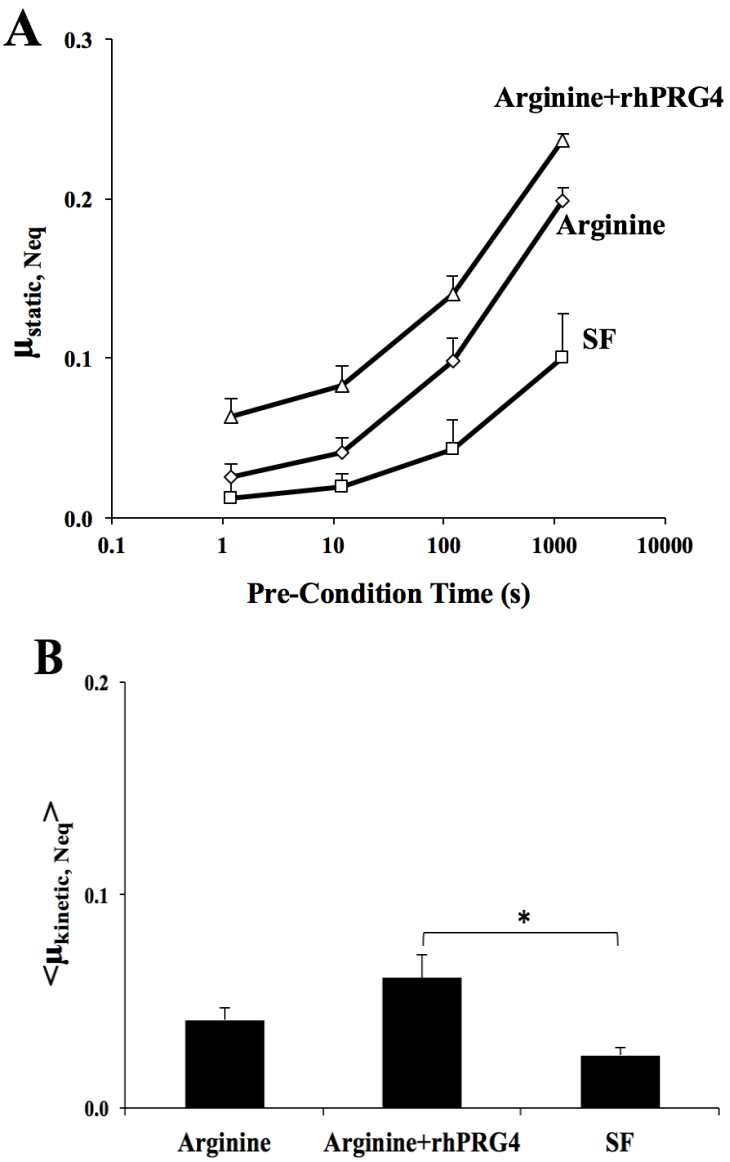

Figure 3-10. Static ($\mu_{static,Neq}$) (**A**) and kinetic ($<\mu_{kinetic,Neq}>$) at Tps = 1.2 s (**B**) friction coefficients of Arginine, Arginine+rhPRG4 and SF with rhPRG4 preparations at 450 μg/mL (N = 4).

3.3.3 Cartilage Boundary Lubricating Ability of Calcium+rhPRG4 Compared to Calcium Alone

The addition of rhPRG4 (450 μg/mL) improved the cartilage boundary lubricating ability of calcium (20 mM). $\mu_{static,Neq}$ varied with Tps and test lubricant ($p < 0.05$) with an interaction ($p = 0.017$). Values increased with Tps and were consistently highest in calcium and lowest in SF,

with the exception of Calcium+rhPRG4 at Tps = 1.2 s being the lowest. Calcium+rhPRG4 was intermediate at Tps = 12, 120, and 1200 s (**Figure 3-11A**).

$<\mu_{kinetic,Neq}>$ values showed similar trends, varying with Tps and test lubricant ($p < 0.05$), increasing only slightly with Tps, with an interaction ($p = 0.006$). At Tps = 1.2 s $<\mu_{kinetic,Neq}>$ was greatest in calcium (0.130 ± 0.019), lowest in SF (0.053 ± 0.005), and intermediate for Calcium+rhPRG4 (0.063 ± 0.004) (**Figure 3-11B**). $<\mu_{kinetic,Neq}>$ was significantly different between calcium and SF ($p = 0.021$).

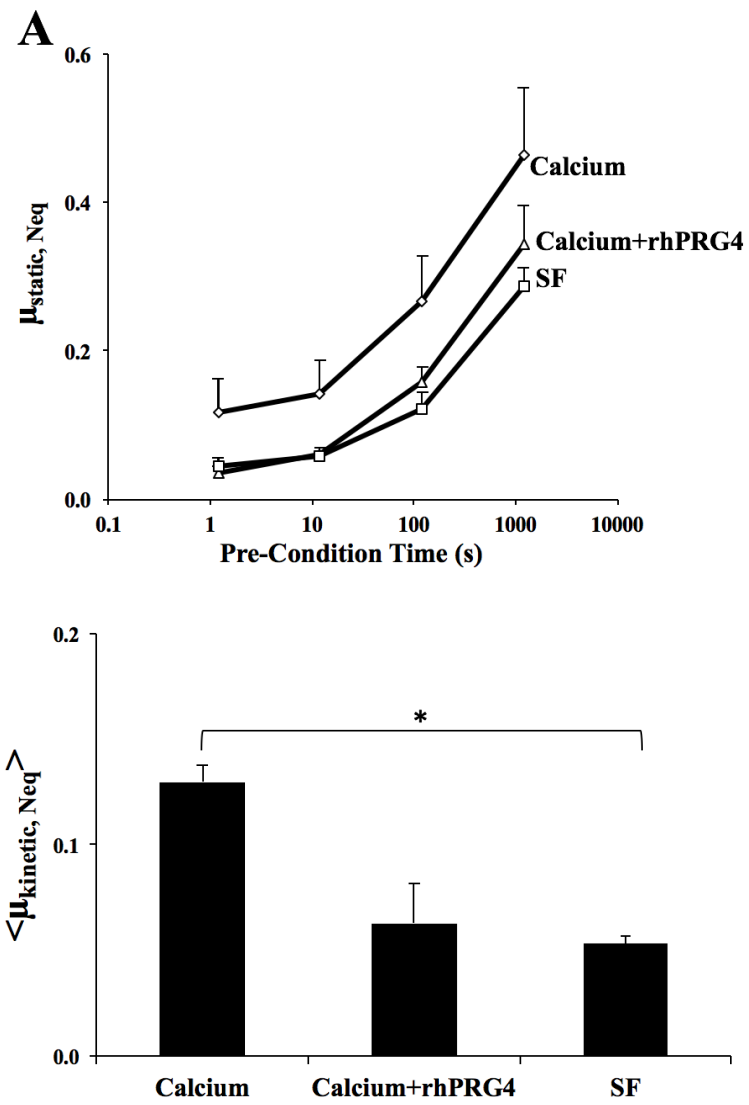

Figure 3-11. Static ($\mu_{static,Neq}$) (**A**) and kinetic ($<\mu_{kinetic,Neq}>$) at Tps = 1.2 s (**B**) friction coefficients of Calcium, Calcium+rhPRG4 and SF with rhPRG4 preparations at 450 μg/mL (N = 4). * denotes $p < 0.05$.

rhPRG4 was able to reduce both the static and kinetic coefficients of friction of PBS at a cartilage-cartilage interface at all pre-sliding durations. Addition of rhPRG4 to arginine resulted in an increase in both static and kinetic at all pre-sliding durations. Addition of rhPRG4 to calcium resulted in a reduction of both static and kinetic friction at all pre-sliding durations. SF was

consistently lowest in all tests. These results are similar to those obtained at a PDMS-glass interface and suggest that the ability of rhPRG4 to form its supramolecular structure is important for its function as a boundary lubricant.

Chapter 4: Discussion

4.1 Effect of Concentration on rhPRG4 Size and Lubricating Ability

Formation of the supramolecular structure of rhPRG4 is most likely mediated through hydrogen bonding, as commonly observed with other proteins [81]. This occurs through the formation of hydrogen bonds via amino acid side chains to form a hydrogen bonded network. However, electrostatic repulsion between negatively charged mucin domains is likely to limit the amount of hydrogen bonding that can occur, which relies on a favourable geometry between adjacent molecules. It is also possible that hydrophobic interactions play a role in mediating the formation of the rhPRG4 supramolecular structure. Since the rhPRG4 end domains are hydrophobic and the central mucin domain is hydrophilic, it is possible that rhPRG4 forms intermolecular aggregates in solution. This would shield the end domains from the polar media, allowing the central domain to interact with the polar media, resulting in the formation of a hydrogen bonded network.

Western blotting showed that rhPRG4 exists as a higher order supramolecular structure. A similar result was previously reported with disulfide-bonded PRG4 dimer and multimers [25][38] [82]. An immunoreactive band around 1048 kDa was observed, as well as immunoreactive species above 1236 kDa in native PAGE. This is consistent with previous studies that identified the apparent MW of PRG4 multimers to range from 1493 – 867 kDa [25][38]. Under denaturing conditions (SDS-PAGE), a high MW species with a distinct immunoreactive band was observed above 460 kDa, as well as a high MW species at the top of the gel. Immunoreactive species were also observed around 460 kDa indicating the presence of monomers. rhPRG4 at 50 and 150 μg/mL demonstrated most of the rhPRG4 species concentrated at the band above 460 kDa. rhPRG4 at 450 μg/mL showed more saturated signal the area above the band ~ 480 kDa. rhPRG4 at 1200 μg/mL

demonstrated more concentration of signal at high apparent MWs compared to 50, 150, and 450 μg/mL near the top of the gel, as well as a band above 460 kDa. This suggests that the rhPRG4 supramolecular structure is dose dependent. The results obtained from Western blotting confirm that a higher order rhPRG4 species is present over concentrations ranging from 50 – 1200 μg/mL and is dose dependent, increasing with concentration.

DLS results also confirmed the presence of a supramolecular structure. The intensity distribution of DLS showed peaks at smaller sizes ranging from ~ 35 to ~ 50 nm in rhPRG4 solutions of concentrations 50, 150, 450, and 1200 μg/mL, which can most likely be attributed to rhPRG4 monomers. This is also observed in the number distribution. The typical hydrodynamic diameter observed for mucin monomers of comparable size is ~ 50 nm [83]. The intensity distribution also indicates the presence of a higher order structure in all rhPRG4 samples with peaks between 200 – 250 nm. The Z-averaged hydrodynamic diameter observed for rhPRG4 at 50, 150, 450, and 1200 μg/mL was 158.90 ± 0.019, 164.31 ± 0.013, 167.00 ± 0.046, and 181.90 ± 0.027 nm respectively. A previous study determined the average hydrodynamic radius of PRG4 (1200 μg/mL) purified from human synovial fluid to be 86 nm (hydrodynamic diameter = 172 nm) [84]. This is within the range of Z – averaged hydrodynamic diameters observed, however is smaller than rhPRG4 of the same concentration. This is because the PRG4 measured in the previous study was determined to be disulfide bonded dimers since the hydrodynamic radius was approximately double that observed for PRG4 monomers [84].It is likely the purification process resulted in removal or alteration of the supramolecular structure. The rhPRG4 aggregates between 200 – 250 nm shown in the intensity distribution are therefore attributed to a higher order structure due to the large increase in size from 172 nm for the disulfide – bonded dimer to ~ 260 nm observed in the intensity distribution for rhPRG4 at the same concentration (1200 μg/mL). The size

distributions also showed rhPRG4 supramolecular formation is concentration dependent as a shift to larger sizes is observed with increasing concentration. Concentration dependency of aggregation has been observed previously in the DLS of proteins with aggregation formation increasing with concentration [85]. The hydrodynamic size of the supramolecular complex of rhPRG4 demonstrates an increase with increasing concentration, however does not increase proportionally with concentration. This suggests that rhPRG4 supramolecular structure is not formed by rhPRG4 molecules interacting end to end, but rather aggregate in a stacking manner. This further suggests interaction of the rhPRG4 mucin domains. The results observed with DLS confirm that rhPRG4 forms its exists in a higher order structure in a dose-dependent manner.

rhPRG4 exhibited a concentration dependency in its ability to reduce friction at a PDMS-glass interface. The results showed a decrease in coefficient of friction with increasing concentration, which is consistent with increased presence of a higher order rhPRG4 structure. A decrease in coefficient of friction was observed between PBS and all concentrations of rhPRG4 at a velocity of 0.398 mm/s, which is within the boundary mode of lubrication [76]. Similar results were observed previously with PRG4 multimers which exhibited a concentration dependency at test concentrations of 45, 150, and 450 μg/mL at a cartilage-cartilage interface [38]. It was also confirmed that rhPRG4 in PBS functions as an effective boundary lubricant ($\mu = 0.052 \pm 0.010$) at a cartilage-cartilage interface. This observation has previously been reported with disulfide-bonded multimers [38]. These results indicate that a solution of rhPRG4 that contains supramolecular structures is able to function as an effective boundary lubricant.

The $<\mu_{kinetic,Neq}>$ measured for PBS, arginine and calcium buffers varied greatly (**Figure 4-1A**). $<\mu_{kinetic,Neq}>$ was highest in calcium (0.130 ± 0.019), lowest in arginine (0.041 ± 0.006) and intermediate in PBS (0.104 ± 0.042). Though the buffers themselves exhibited a large amount of

variation in $<\mu_{kinetic,Neq}>$ values, when rhPRG4 was added large deviations in these values were not observed between buffers (**Figure 4-1B**). $<\mu_{kinetic,Neq}>$ was highest in calcium+rhPRG4 (0.063 ± 0.004), lowest in PBS+rhPRG4 (0.052 ± 0.010) and intermediate in arginine+rhPRG4 (0.061 ± 0.011)

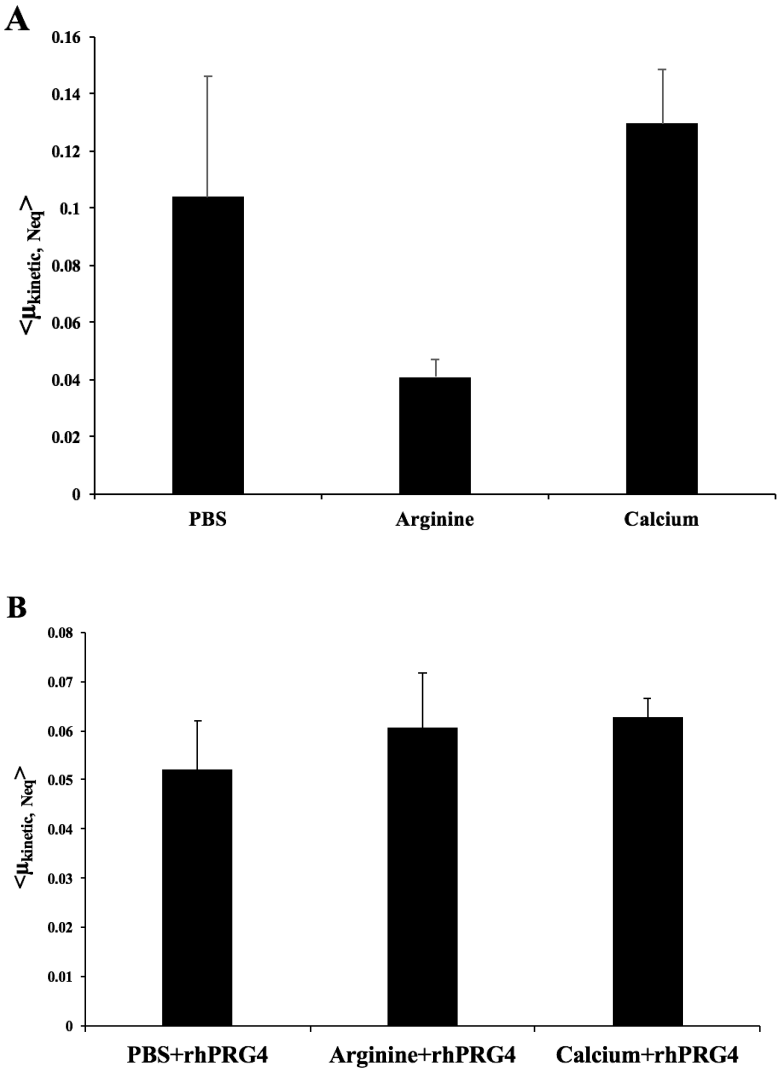

Figure 4-1. Kinetic $<\mu_{kinetic, Neq}>$ coefficient of friction at Tps = 1.2 s of (A) buffer solutions and (B) buffers with rhPRG4 (450 μg/mL) added.

4.2 Effect of Arginine on rhPRG4 Size and Lubricating Ability

Arginine is commonly used to suppress protein-protein interactions in pharmaceutical formulations, and therefore decrease aggregation. Arginine interacts with aromatic and charged residues on proteins through cation-π, hydrogen bonding, and hydrophobic interactions [61]. Since rhPRG4 in abundant in charged residues and also contains aromatic residues there are many potential sites for interaction with arginine. The interaction of arginine with proteins is limited due to its larger size compared to other aggregation suppressants such as guanidine. Arginine is able to self-assemble into larger structures such as dimers and trimers [61]. This occurs through hydrogen bonding between adjacent carboxylate and guandinium groups on arginine molecules [61]. The ability of arginine to self-associate is concentration dependent, with hydrogen bonding increasing with concentration [61]. The formation of these larger arginine clusters limits arginine's interaction with proteins to the protein surface [61]. Since arginine interaction with proteins is limited to the protein surface this is most likely why arginine does not cause protein denaturation as is observed with guanidine [59][61]. Arginine interacts with proteins mainly through its guanidinium group and it able to interact with both positively and negatively charged amino acid side chains [61].

Hydrogen bond formation between arginine and rhPRG4 most likely occurs through the carboxylate group of sialic acid residues on rhPRG4 and the guanidinium group on arginine. This is similar to the arginine-arginine hydrogen bond formation that has been observed previously [61]. Arginine is also able to interact with aromatic side chains to form cation-π interactions. rhPRG4 contains tyrosine and phenylalanine, which can serve as potential sites for interaction with arginine. This occurs via the cationic side chain of arginine and aromatic side chain of either phenylalanine or tyrosine. This type of interaction requires a very specific geometry with the cationic and aromatic group being oriented parallel to one another [55]. Therefore, it is unlikely

that this type of interaction is as prevalent as hydrogen bonding. Finally, arginine is also able to interact with hydrophobic residues on proteins. This occurs via the methylene groups in arginine and the hydrophobic residues on the protein surface. The end domains of rhPRG4 are abundant in cysteine and therefore hydrophobic. Though arginine is able to interact with rhPRG4 through hydrophobic interactions, it is unlikely that this type of interaction is very strong since in native protein structures the hydrophobic residues are oriented away from the solvent and not accessible to the large arginine molecules [61].

The collective effects of these putative interactions between arginine and rhPRG4 were observed in western blotting and DLS. Western blotting of rhPRG4 in 0.2 M arginine demonstrated a change in supramolecular structure. Compared to rhPRG4 in PBS there was redistribution in signal with the same amount of rhPRG4 loaded. There was a decrease in the presence of a higher order structure, which can be seen by a decreased signal at MWs of 1048 kDa and above in native PAGE with mAb 9G3 which binds to the mucin domain of rhPRG4. Similar results were also observed with antibody anti-PRG4 LPN, which recognizes the C – terminal of rhPRG4. Binding of LPN showed almost no signal compared to rhPRG4 in PBS and calcium. DLS measurements determined the average hydrodynamic size of particles to be 147.5 nm. This is a decrease in size from 164.02 nm of rhPRG4 in PBS. DLS also complemented western blot results, demonstrating that although the supramolecular structure was still there in the presence of arginine it was less abundant than in PBS. This is best demonstrated by the intensity distribution where the peak at ~ 38 nm is stronger in arginine than for PBS, and the peak corresponding to rhPRG4 aggregates at ~ 200 nm is reduced in arginine compared to PBS. The change in rhPRG4 supramolecular size in the presence of arginine further confirms that this structure is mediated through non-covalent

interactions since the same interactions that would occur between adjacent rhPRG4 molecules instead occurs between rhPRG4 and arginine.

Friction testing at a PDMS-glass interface showed an increase in coefficient of friction of arginine when rhPRG4 was added. rhPRG4 in arginine also resulted in higher coefficients of friction compared to rhPRG4 in PBS in boundary lubrication mode. Similar results were observed at a cartilage-cartilage interface where addition of rhPRG4 resulted in an increase in the kinetic coefficient of friction of a 0.2 M arginine solution from 0.061 ± 0.011 from 0.041 ± 0.006. The kinetic coefficient of friction of rhPRG4 in arginine was also higher than that observed for rhPRG4 in PBS (0.052 ± 0.010). This suggests that the ability of rhPRG4 to form its supramolecular structure is important for its ability to function as an effective boundary lubricant as its diminished ability to do so in arginine resulted in an increase in *in vitro* friction.

4.3 Effect of Calcium on rhPRG4 Size and Lubricating Ability

The results of this thesis indicate that calcium enhances the formation of the supramolecular structure of rhPRG4. Calcium's ability to rearrange the structural organization of macromolecules has been observed before. When calcium is added to salivary mucus (MUC5B) it induces a structural change that causes the pores of MUC5B to shrink and MW to increase. This is due to aggregates of MUC5B monomers through intermolecular cross-links mediated by calcium. It is likely that rhPRG4 behaves in a similar manner. Calcium has a high affinity for the negative charge on sialic residues, which are abundant in rhPRG4, and is therefore a site for formation of calcium-ion bridges. The binding of calcium ions to sialic residues has been observed before in facilitating the assembly of glycoprotein complexes [35]. It has been also shown previously that calcium has an effect on structure of self-assembled PRG4 layers using 89 % pure bovine PRG4 from SF [35]. Calcium ions are able to shed their hydration layer relatively easily and able to form calcium-ion

bridging interactions where calcium ions form ionic bonds with two anions located on adjacent charged macromolecules or within different regions of a single macromolecule [35]. Calcium is able to lower electrostatic repulsion between molecules which usually prevents the molecules from approaching close enough to bond. Due to the large number of sialic residues on rhPRG4 it is possible that each molecule has the ability to form multiple calcium ion bridges leading to the formation of a branched supramolecular structure.

Western blotting with mAb 9G3 demonstrated an increase in supramolecular structure compared to PBS. While PBS showed a majority of immunoreactive species around 1048 kDa, the abundance of signal in calcium was at the top of the gel in native PAGE. Similar results were observed with Ab LPN, which showed a very strong band at the very top of the gel. This band was much stronger in calcium compared to PBS and arginine. An additional band was observed at ~ 1236 kDa which was stronger in calcium compared to PBS and not present in arginine. Therefore, western blotting confirmed the presence of a higher order structure and suggests that calcium helps enhance the formation of rhPRG4's higher order structure. This was also confirmed in DLS. Both the number and intensity distributions confirm the presence of rhPRG4 aggregates at ~ 459 and ~ 712 nm respectively. These aggregates are present in PBS and arginine at ~ 220 nm, which is considerably smaller. This Z-average for rhPRG4 in calcium was determined to be 664.02 ± 56.90 nm which is significantly larger than that of rhPRG4 in either PBS or arginine.

These experiments were performed at a concentration of 20 mM of calcium, which is considerably higher than the normal concentration of ~ 5 mM calcium in SF [35]. A previous study of the exposure of self-assembled bovine PRG4 layers to calcium showed that calcium exhibited a concentration dependency [35]. At 5 mM calcium did not have any effect on the structure of self-assembled PRG4 layers, however at 20 mM a change was observed [35]. While the results of this

thesis show that calcium is able to mediate the formation of the supramolecular structure of rhPRG4, it is unknown it if is able to do so at lower concentrations similar to that observed physiologically or a concentration between 5 and 20 mM. It is also possible higher concentrations of calcium above 20 mM could result in even more supramolecular formation. It is unknown if the formation of ion bridges is specific to calcium, or if they can occur in the presence of other divalent ions such as Mg^{2+}, or Fe^{2+}, or even trivalent ions. Calcium mediated protein interactions with other mucins, such as MUC5B and submaxillary gland mucus has been shown to be calcium dependent and was not observed in the presence of manganese, zinc [58] or magnesium [58][86]. Therefore, it is possible that the effects observed in rhPRG4 structure may be calcium dependent as well.

Friction testing at a PDMS-glass interface showed that addition of rhPRG4 to a 20mM calcium solution lowered the coefficient of friction of calcium. This reduction in friction was statistically significant at 0.398 and 3.98 mm/s, indicating that rhPRG4 in calcium functions as an effective boundary lubricant. Similar results were observed at a cartilage-cartilage interface. The addition of rhPRG4 to calcium lowered the kinetic coefficient of friction from 0.13 ± 0.019 to 0.063 ± 0.004.

The ability of rhPRG4 to form its supramolecular structure in OA is unknown. Calcium concentrations in OA are not typically reported, however common to joint disease and injury include the demineralization of the calcified cartilage zone and appearance of calcium pyrophosphate suggesting these conditions result in increased calcium [35]. Since calcium was shown to have a high coefficient of friction at a cartilage-cartilage interface, an increased calcium concentration in the synovial joint could result in increased friction and further wear of the joint. It is possible that administration of rhPRG4 could help reduce friction in OA as calcium would be

attracted to rhPRG4 due to its sialic residues and form the supramolecular structure, decreasing both the amount of free calcium ions in the joint and therefore friction.

4.4 Limitations

While this work contributes to the understanding of the supramolecular formation of rhPRG4 and its structure – function relationship, there are several limitations, that while they do not change the conclusions drawn from the study, should be acknowledged. A limitation of DLS is that determination of hydrodynamic size is more optimal when samples are monodisperse, meaning there is only one particle size in the test solution [85]. This results in a more accurate Z-average. Since the Z-average is weighted towards the presence of aggregates, the Z-average reported may be skewed to larger sizes even when the aggregates are present in very small quantities. In monodisperse samples only one peak is observed thereby giving a more accurate hydrodynamic size. Because of this, DLS is often used to screen for the presence of aggregates rather than determine their size. This could be remedied by using another experimental technique such as high-performance liquid chromatography (HPLC) with a size exclusion column to separate the different sized particles in solution. The different fractions obtained from HPLC could then be measured separately using DLS allowing for determination of a true hydrodynamic radius. Pilot work using this method to separate PRG4 has indicated that obtaining reproducible data is difficult, requiring at least 20 sample injections to precondition the column, since there are column interactions with rhPRG4. This results in carry over of sample between injections. Though the Z-average may not represent the true hydrodynamic size of rhPRG4, it allows for a clear comparison of rhPRG4 particles sizes which varied with both concentration and buffer. Another potential limitation of DLS is the assumptions used to transform the intensity distribution to the number distribution. The number distribution is useful to compare the size of rhPRG4 particles in solution

since it is directly proportional to size, while the intensity distribution is useful for detecting small amounts of aggregates. Therefore, all sizes are reported as determined from the intensity distribution which does not require these assumptions. Finally, a nanosphere of known size could be measured in buffer first to determine the Zetasizer is calibrated correctly and the viscosity and refractive index values used for the buffer rhPRG4 is immersed in are accurate.

Another limitation of this project is that arginine is basic. It is possible when added to PBS arginine increased its pH. At physiological pH arginine is protonated and therefore carries a positive charge. It is possible that these experiments were conducted at a pH that is above that observed physiologically and arginine may not have been protonated and positively charged. Therefore, the pH of the arginine buffer should be measured prior to experiments with rhPRG4. In addition to measuring the buffer pH, the effect of basic pH on rhPRG4 supramolecular structure and function in the absence of arginine could also be studied. This would determine if changes in rhPRG4 structure and function occur due to arginine or the basicity of the buffer.

A limitation of friction testing at both a cartilage-cartilage and PDMS-glass interface is that they do not represent the whole joint where multiple modes of lubrication are acting. However, they allow for isolation of the boundary lubrication mode where rhPRG4 functions as a boundary lubricant. Another potential limitation of friction testing at a cartilage-cartilage interface is that this test is technically challenging to complete. Lubrication testing was done in order of presumed increasing lubricating function in order to eliminate any potential carry over between test lubricants. Friction testing at a PDMS-glass interface uses synthetic surfaces which may not result in physiologically relevant results; however, it allows for classic Stribeck analysis with varying velocity which cannot be done with soft, permeable materials. This is because the lubrication of a soft, porous material such as articular cartilage is more complex and does not generate a normal

Stribeck curve. Though a PDMS-glass interface may not yield physiologically relevant results, PRG4 has been studied successfully at various interfaces, including at cartilage-cartilage [24][79], cartilage-glass [79], and latex-glass [78], suggesting these results may be relevant.

Chapter 5: Conclusions

5.1 Summary of Findings

The findings of this thesis show that rhPRG4 exists as a higher order supramolecular structure that is mediated through non-covalent interactions. The presence of this structure is confirmed through western blotting and DLS which showed the presence of a higher order MW structure and rhPRG4 aggregation respectively. The formation of the supramolecular structure is likely mainly through the formation of hydrogen bonds between adjacent rhPRG4 molecules, although hydrophobic interactions may also play a role. The Z-average of rhPRG4 in PBS was determined to be 166.02 ± 3.80 nm, which was statistically significantly smaller than that measured in 20mM calcium, but not 0.2M arginine. DLS and friction testing at a PDMS-glass interface showed that the formation of the supramolecular structure is concentration dependent with size and lubricating increasing with increasing concentration. At a PDMS-glass interface, rhPRG4 in PBS resulted in a statistically significant decrease in coefficient of friction at a velocity of 0.398 mm/s at concentrations of 50, 150, 450, and 1200 μg/mL. The coefficient of friction showed a trend of decreasing with increasing rhPRG4 concentrations. rhPRG4 in PBS was also able to function as an effective boundary lubricant at a cartilage-cartilage interface, reducing the kinetic coefficient of friction of PBS from 0.104 ± 0.042 to 0.052 ± 0.010. The addition of rhPRG4 to PBS also reduced the static coefficient of friction at each pre-sliding duration.

Arginine demonstrated the ability to disrupt the formation of the rhPRG4 supramolecular structure. This occurs most likely through the formation of hydrogen bonds between the guanidinium group on arginine and the carboxylate groups on rhPRG4. Cation-π, and hydrophobic interactions may also play a role in disrupting the formation of this higher order structure. This could be explained by arginine occupying the same sites on rhPRG4 that would otherwise be

involved in the formation of the supramolecular structure, thereby preventing protein-protein interaction. This was confirmed through western blotting and DLS. Western blotting showed a decrease in signal and presence of a high MW fragment compared to rhPRG4 in PBS. DLS also showed a decrease in the supramolecular structure with a shift to smaller sizes in the size distribution measurements compared to PBS. The Z-average of rhPRG4 in arginine was 147.50 ± 3.90, which was lower than that observed with PBS. Friction testing at a PDMS-glass interface demonstrated an increase in coefficient of friction in 0.2 M arginine upon the addition of rhPRG4. At a cartilage-cartilage interface the addition of rhPRG4 to arginine also resulted in an increase in kinetic coefficient of friction from 0.041 ± 0.006 to 0.061 ± 0.011. An increase in static coefficient of friction was also observed at each pre-sliding duration.

Calcium demonstrated the ability to enhance the formation of the rhPRG4 supramolecular structure. This most likely occurs through the formation of calcium-ion bridges between calcium and the carboxylate groups on the sialic acid residues of rhPRG4. Western blotting and DLS confirmed the presence of the supramolecular structure. Western blots showed greater signal at high apparent MWs indicating there was more of the supramolecular structure of rhPRG4 when in 20 mM calcium than PBS. DLS demonstrated similar results with the presence of a peak at ~ 712 nm in the intensity distribution indicating the formation of larger protein aggregates compared to ~ 220 nm as is seen with PBS. The Z-average for calcium was determined to be 664.02 ± 56.90 nm which is statistically significantly higher than the values of 164.02 ± 3.80 nm and 147.50 ± 3.90 nm that were observed for PBS and arginine respectively. Friction testing at a PDMS-glass interface showed that rhPRG4 resulted in a decreased in the coefficient of friction of calcium across all velocities, and this decrease was significant at velocities of 0.398 and 3.98 mm/s. Similar results were observed with friction testing at a cartilage-cartilage interface. The addition of

rhPRG4 to 20 mM calcium resulted in a reduction in the kinetic coefficient of friction from 0.130 ± 0.019 to 0.063 ± 0.004. rhPRG4 was also able to reduce the static coefficient of friction of calcium at each pre-sliding duration.

Collectively the findings of this thesis demonstrate that rhPRG4 exists as a supramolecular structure that is mediated through non-covalent interactions. The formation of the rhPRG4 supramolecular structure is dose dependent, increasing with concentration, and can be altered by arginine and calcium. Arginine (0.2 M) disrupted the formation of the supramolecular structure most likely through hydrogen bonding between the guanidinium group on arginine and carboxylate groups on rhPRG4. This causes arginine to occupy sites that other rhPRG4 molecules would otherwise bind to suppressing protein-protein interaction. Calcium (20 mM) enhanced the formation of the supramolecular structure most likely through the formation of calcium-ion bridges. These interactions decrease electrostatic repulsion between rhPRG4 molecules allowing them to interact. Friction testing at both a PDMS-glass and a cartilage-cartilage interface showed that altered proportions of the rhPRG4 supramolecular structure can affect the lubricating ability of rhPRG4, though this was also affected by the buffer itself as arginine lubricated well on its own and calcium did not. These findings further contribute to the understanding of PRG4's structure – function relationship.

5.2 Future Work

To fully understand the interaction that calcium has with rhPRG4 further experiments are required. These include experiments to determine if a) the observed effect with calcium is reversible (with the use of a chelating agent), b) if other metal ions result in a similar ion-bridging interaction, c) if the effect observed with calcium is dose dependent and d) if other calcium compounds exhibit similar effects. Calcium interactions with proteins resulting in change in

structure and function has been observed previously to be reversible [35][58]. The structural organization observed in salivary mucus, MUC5B, was reversed with the addition of a chelating agent, ethylene glycol-bis(2-aminoethylether)-N,N,N',N'-tetraacetic acid (EGTA). This suggested that EGTA was chelating calcium resulting in reversibility of the structural rearrangement induced by calcium. Similar results were also observed in self-assembled lubricin layers [35]. The exposure of self-assembled lubricin layers to calcium resulted in a change in both the structure and properties of these layers. The exchange of calcium with PBS resulted the structure and properties to revert back to those observed with PBS indicating the calcium ion interactions were fully reversible [35]. Therefore, further experiments could be done to determine if the observed enhanced formation of the supramolecular structure of calcium is reversible with chelating agents such as ethylenediaminetetraacetic acid (EDTA). It remains unknown if the putative ion bridging interactions observed with rhPRG4 are calcium dependent, or if the same results would be observed with other divalent metal ions. Similar ion-bridging interactions with calcium observed in other mucins were determined to be calcium dependent [58][86]. Therefore, to fully understand this phenomena future experiments could include size measurements of rhPRG4 after exposing rhPRG4 to another divalent ion such as magnesium to observe if the same increase in size occurs. The effect of calcium on formation of the rhPRG4 supramolecular structure could be dose dependent. The calcium used in these experiments was at a concentration of 20 mM, which is much greater than the physiological concentration in SF of ~ 5 mM. It is possible that calcium could elicit the same response in formation of the supramolecular structure at a concentration between 5 and 20 mM. If calcium is able to enhance the formation of the supramolecular structure at a lower concentration it is possible that the kinetic coefficient of friction of 0.063 ± 0.004 that was observed may be lowered, as calcium itself exhibits a high coefficient of friction thereby

increasing that of rhPRG4. Finally, the effect of other calcium compounds and their effect on rhPRG4 structure and lubricating ability could be studied. In these experiments calcium chloride was used to make the calcium buffer. Calcium chloride has been used previously to determine the effects of calcium of PRG4 [35] and other mucins [58]. However, it is possible the use of other calcium compounds such as calcium sulfate could elicit a different effect than that observed with calcium chloride.

Dynamic light scattering is a common method for measuring protein size, however as mentioned previously there are limitations when working with polydisperse solutions such a rhPRG4. A more accurate protein size could be determined by separating the proteins first before analyzing via DLS. This is commonly done by high performance liquid chromatography – size exclusion chromatography (HPLC-SEC) with multi-angle light scattering (MALLS). MALLS is a non-destructive analytical techniques that allows for accurate determination of molecular size and mass and can be used to characterize proteins and aggregates with high MWs [25]. HPLC-SEC with MALLS has been used previously for the separation and MW characterization of bovine PRG4 [25]. This would allow for collection of fractions each with a different protein size and DLS could be used to analyze each size separately, resulting in a more accurate hydrodynamic size. However, this would require the development of an appropriate protocol for using HPLC-SEC with rhPRG4 as obtaining reproducible data is difficult since rhPRG4 has been observed to interact with column resins resulting in carryover of sample injections and difficulty conditioning the column. In addition to HPLC-SEC with MALLS to more accurately determine the weight of the rhPRG4 supramolecular structure, another method such as mass spectrometry could be used as an alternative to western blotting. Though western blotting is useful in the detection of the supramolecular structure of rhPRG4, the MW obtained is an apparent MW, which tends to be

larger than the actual MW. This is because rhPRG4 is able to bind SDS which increases the size of the protein and alters its mobility through the gel leading to increased MWs. However, since native PAGE is done in the absence of SDS it results in a more accurate MW.

Further experiments could also be done to determine the effect of supramolecular structure and buffer on rhPRG4's ability to interact with HA. The interaction of PRG4 and HA had been shown to be important as these two synovial fluid constituents act synergistically to reduce friction [2][26][87][88]. The ability of PRG4 to interact with HA is important in achieving the ultra-low coefficient of friction that is characteristic of synovial joints. It has been shown that rhPRG4 is interacts with HA to achieve these low coefficient of friction values [26], however the effect of the supramolecular structure on rhPRG4's ability to interaction with HA remains to be fully elucidated. It has been shown previously that the exposure of rhPRG4 to a detergent, CHAPS, altered PRG4's ability to interact with HA, resulting in decreased lubricating ability at a cartilage-cartilage interface [89]. It is possible that the presence of arginine or calcium could exhibit a similar effect, altering rhPRG4's ability to interact with HA resulting in diminished lubrication. Similarly, the effect of the supramolecular structure on rhPRG4's ability to adhere to the cartilage surface has not yet been investigated. rhPRG4 itself has been shown to adhere to the cartilage surface in a manner similar to PRG4 and SF [26]. The interaction of the supramolecular structure of rhPRG4 and its ability to interact with HA, as well as its ability to adhere to the cartilage surface are both critical properties in the development of a potential biotherapeutic. It is possible that the supramolecular structure of rhPRG4 could be useful in the formulation of an intraarticular injection for OA treatment. It has been shown in a pre-clinical large animal model that IA injections of rhPRG4 after medial meniscus destabilization (DMM) resulted in less macroscopic cartilage damage [51]. If the supramolecular structure of rhPRG4 is shown to be able to act synergistically

with HA, it is possible that an altered formulation of the IA injections that enhanced the supramolecular structure could improve the in vivo outcomes in pre-clinical models of OA.

References

[1] V. C. Mow, G. A. Ateshian, and R. L. Spilker, "Biomechanics of Diarthrodial Joints: A Review of Twenty Years of Progress," *J. Biomech. Eng.*, vol. 115, no. 4B, p. 460, 1993.

[2] S. E. Majd, R. Kuijer, A. Köwitsch, T. Groth, T. A. Schmidt, and P. K. Sharma, "Both hyaluronan and collagen type II keep proteoglycan 4 (lubricin) at the cartilage surface in a condition that provides low friction during boundary lubrication," *Langmuir*, vol. 30, no. 48, pp. 14566–14572, 2014.

[3] G. a Ateshian, V. C. Mow, and R. Huiskes, "Friction, lubrication, and wear of articular cartilage and diarthrodial joints," in *Basic Orthopaedic Biomechanics & Mechano-Biology*, 3rd ed., vol. 3rd, V. C. Mow and R. Huiskes, Eds. Philadelphia: Lippincott Williams & Wilkins, 2005, pp. 447–494.

[4] A. J. Sophia Fox, A. Bedi, and S. A. Rodeo, "The basic science of articular cartilage: Structure, composition, and function," *Sports Health*, vol. 1, no. 6, pp. 461–468, 2009.

[5] J. A. Buckwalter and H. A. Mankin, "Instructional course lectures, the american academy of orthopaedic surgerons - Articular Cartilage part I: tissue design and chondrocyte-matrix interactions," *J. Bone Jt. Surg.*, 1997.

[6] N. Gerwin, C. Hops, and A. Lucke, "Intraarticular drug delivery in osteoarthritis," *Adv. Drug Deliv. Rev.*, vol. 58, no. 2, pp. 226–242, 2006.

[7] J. A. Buckwalter, H. A. Mankin, and A. J. Grodzinsky, "Articular cartilage and osteoarthritis," *AAOS Instr. Course Lect.*, vol. 54, pp. 465–480, 2005.

[8] L. Han, A. J. Grodzinsky, and C. Ortiz, "Nanomechanics of cartilage extracellular matrix," *Annu. Rev. Mater. Res.*, vol. 41, pp. 133–168, 2011.

[9] M. E. Blewis, G. E. Nugent-Derfus, T. A. Schmidt, B. L. Schumacher, and R. L. Sah, "A model of synovial fluid lubricant composition in normal and injured joints," *Eur. Cells Mater.*, vol. 13, no. 858, pp. 26–38, 2007.

[10] A. Y. Hui and W. J. Mccarty, "A systems biology approach to synovial joint lubrication in health, injury, and disease," *Wiley Interdiscip Rev Syst Biol Med*, vol. 4, no. 1, pp. 15–37, 2012.

[11] J. Buckwalter, V. Mow, and A. Ratcliffe, "Restoration of Injured or Degenerated Articular Cartilage.," *J. Am. Acad. Orthop. Surg.*, vol. 2, no. August 1994, pp. 192–201, 1994.

[12] T. A. Schmidt, N. S. Gastelum, E. H. Han, G. E. Nugent-Derfus, B. L. Schumacher, and R. L. Sah, "Differential regulation of proteoglycan 4 metabolism in cartilage by IL-1α, IGF-I, and TGF-β1," *Osteoarthr. Cartil.*, vol. 16, no. 1, pp. 90–97, 2008.

[13] J. P. Gleghorn, A. R. C. Jones, C. R. Flannery, and L. J. Bonassar, "Boundary mode frictional properties of engineered cartilaginous tissues," *Eur. Cells Mater.*, vol. 14, pp. 20–28, 2007.

[14] J. P. Gleghorn and L. J. Bonassar, "Lubrication mode analysis of articular cartilage using Stribeck surfaces," *J. Biomech.*, vol. 41, no. 9, pp. 1910–1918, 2008.

[15] M. Daniel, "Boundary cartilage lubrication: Review of current concepts," *Wiener*

Medizinische Wochenschrift, vol. 164, pp. 88–94, 2014.
[16] J. M. Coles, D. P. Chang, and S. Zauscher, "Molecular mechanisms of aqueous boundary lubrication by mucinous glycoproteins," *Curr. Opin. Colloid Interface Sci.*, vol. 15, no. 6, pp. 406–416, 2010.
[17] E. D. Bonnevie, D. Galesso, C. Secchieri, I. Cohen, and L. J. Bonassar, "Elastoviscous transitions of articular cartilage reveal a mechanism of synergy between lubricin and hyaluronic acid," *PLoS One*, vol. 10, no. 11, pp. 1–15, 2015.
[18] G. D. Jay and K. A. Waller, "The biology of Lubricin: Near frictionless joint motion," *Matrix Biol.*, vol. 39, pp. 17–24, 2014.
[19] G. D. Jay *et al.*, "Association between friction and wear in diarthrodial joints lacking lubricin," *Arthritis Rheum.*, vol. 56, no. 11, pp. 3662–3669, 2007.
[20] T. A. Schmidt and R. L. Sah, "Effect of synovial fluid on boundary lubrication of articular cartilage," *Osteoarthr. Cartil.*, vol. 15, no. 1, pp. 35–47, 2007.
[21] K. Boettcher, S. Grumbein, U. Winkler, J. Nachtsheim, and O. Lieleg, "Adapting a commercial shear rheometer for applications in cartilage research," *Rev. Sci. Instrum.*, vol. 85, no. 9, 2014.
[22] E. D. Bonnevie, C. Secchieri, D. Galesso, and L. J. Bonassar, "Stribeck Analysis Of Synovial Lubricants : Lubricating Mechanisms And Interaction Of Hyaluronic Acid And Lubricin," *Trans Orthop Res Soc*, p. Poster No:0437, 2014.
[23] A. C. Dunn, W. G. Sawyer, and T. E. Angelini, "Gemini interfaces in aqueous lubrication with hydrogels," *Tribol. Lett.*, vol. 54, no. 1, pp. 59–66, 2014.
[24] T. A. Schmidt and R. L. Sah, "Effect of synovial fluid on boundary lubrication of articular cartilage," *Osteoarthr. Cartil.*, vol. 15, no. 1, pp. 35–47, 2007.
[25] B. L. Steele, M. C. Alvarez-Veronesi, and T. A. Schmidt, "Molecular weight characterization of PRG4 proteins using multi-angle laser light scattering (MALLS)," *Osteoarthr. Cartil.*, vol. 21, no. 3, pp. 498–504, 2013.
[26] S. Abubacker, S. G. Dorosz, D. Ponjevic, G. D. Jay, J. R. Matyas, and T. A. Schmidt, "Full-Length Recombinant Human Proteoglycan 4 Interacts with Hyaluronan to Provide Cartilage Boundary Lubrication," *Ann. Biomed. Eng.*, vol. 44, no. 4, pp. 1128–1137, 2016.
[27] G. D. Jay, U. Tantravahi, D. E. Britt, H. J. Barrach, and C. J. Cha, "Homology of lubricin and superficial zone protein (SZP): Products of megakaryocyte stimulating factor (MSF) gene expression by human synovial fibroblasts and articular chondrocytes localized to chromosome 1q25," *J. Orthop. Res.*, vol. 19, no. 4, pp. 677–687, 2001.
[28] S. Basit, Z. Iqbal, M. Umicevic-mirkov, and K. U. Naqvi, "A novel deletion mutation in proteoglycan-4 underlies camptodactyly-arthropathy-coxa-vara-pericarditis syndrome in a consanguineous pakistani family," *Arch. Med. Res.*, vol. 42, no. 2, pp. 110–114, 2011.
[29] M. L. Samsom *et al.*, "Characterization of full-length recombinant human Proteoglycan 4 as an ocular surface boundary lubricant," *Exp. Eye Res.*, vol. 127, pp. 14–19, 2014.
[30] D. Swan and E. Radin, "The Molecular Basis of Articular Lubrication," *J. Biol. Chem.*, vol. 247, no. 24, pp. 8069–8073, 1972.
[31] D. A. Swann, S. Sotman, M. Dixon, and C. Brooks, "The isolation and partial characterization of the major glycoprotein (LGP-I) from the articular lubricating fraction from bovine synovial fluid.," *Biochem. J.*, vol. 161, no. 3, pp. 473–85, 1977.
[32] D. A. Swann, H. S. Slayter, and F. H. Silver, "The molecular structure of lubricating glycoprotein-1, the boundary lubricant of articular cartilage.," *J. Biol. Chem.*, vol. 256, no. 11, pp. 5921–5925, 1981.

[33] D. A. Swann, K. J. Bloch, D. Swindell, and E. Shore, “The lubricating activity of human synovial fluid glycoproteins,” *Arthritis Rheum.*, vol. 24, no. 1, pp. 552–556, 1981.
[34] B. L. Schumacher, J. A. Block, T. M. Schmid, M. B. Aydelotte, and K. E. Kuettner, “A novel proteoglycan synthesized and secreted by chondrocytes of the superficial zone of articular cartilage,” *Arch. Biochem. Biophys.*, vol. 311, no. 1, pp. 144–152, 1994.
[35] G. W. Greene, R. Thapa, S. A. Holt, X. Wang, C. J. Garvey, and R. F. Tabor, “Structure and property changes in self-assembled lubricin layers induced by calcium ion interactions,” *Langmuir*, vol. 33, no. 10, pp. 2559–2570, 2017.
[36] G. D. Jay, “Lubricin and surfacing of articular joints,” *Curr Opin Orthop*, vol. 15, no. 5, pp. 355–359, 2004.
[37] D. P. Chang *et al.*, “Friction force microscopy of lubricin and hyaluronic acid between hydrophobic and hydrophilic surfaces,” *Soft Matter*, vol. 5, no. 18, p. 3438, 2009.
[38] S. Abubacker, D. Ponjevic, H. O. Ham, P. B. Messersmith, J. R. Matyas, and T. A. Schmidt, “Effect of disulfide bonding and multimerisation on Proteoglycan 4’s cartilage boundary lubricating ability and adsorption.,” *Connect. Tissue Res.*, vol. 57, no. 2, pp. 113–123, 2015.
[39] T. A. Schmidt, A. H. K. Plaas, and J. D. Sandy, “Disulfide-bonded multimers of proteoglycan 4 (PRG4) are present in normal synovial fluids,” *Biochim. Biophys. Acta - Gen. Subj.*, vol. 1790, no. 5, pp. 375–384, 2009.
[40] D. K. Rhee *et al.*, “The secreted glycoprotein lubricin protects cartilage surfaces and inhibits synovial cell overgrowth,” *J. Clin. Invest.*, vol. 115, no. 3, pp. 622–631, 2005.
[41] T. A. Schmidt, N. S. Gastelum, Q. T. Nguyen, B. L. Schumacher, and R. L. Sah, “Boundary lubrication of articular cartilage: Role of synovial fluid constituents,” *Arthritis Rheum.*, vol. 56, no. 3, pp. 882–891, 2007.
[42] K. a Waller, L. X. Zhang, K. a Elsaid, B. C. Fleming, M. L. Warman, and G. D. Jay, “Role of lubricin and boundary lubrication in the prevention of chondrocyte apoptosis.,” *Proc. Natl. Acad. Sci. U. S. A.*, vol. 110, no. 15, pp. 5852–7, 2013.
[43] S. Basit *et al.*, “A Novel Deletion Mutation in Proteoglycan-4 Underlies Camptodactyly-Arthropathy-Coxa-Vara-Pericarditis Syndrome in a Consanguineous Pakistani Family,” *Arch. Med. Res.*, vol. 42, no. 2, pp. 110–114, 2011.
[44] M. C. Alvarez-Veronesi, J. Kooyman, and T. A. Schmidt, “Synthesis of proteoglycan-4 (PRG4) disulfide-bonded multimers by chondrocytes in cartilage explants,” *Trans Orthop Res Soc*, p. Poster No: 850, 2010.
[45] Z. Cui, C. Xu, X. Li, J. Song, and B. Yu, “Treatment with recombinant lubricin attenuates osteoarthritis by positive feedback loop between articular cartilage andsubchondral bone in ovariectomized rats,” *Bone*, vol. 74, pp. 37–47, 2015.
[46] C. R. Flannery *et al.*, “Prevention of cartilage degeneration in a rat model of osteoarthritis by intraarticular treatment with recombinant lubricin,” *Arthritis Rheum.*, vol. 60, no. 3, pp. 840–847, 2009.
[47] T. E. Ludwig, J. R. McAllister, V. Lun, J. P. Wiley, and T. A. Schmidt, “Diminished cartilage-lubricating ability of human osteoarthritic synovial fluid deficient in proteoglycan 4: Restoration through proteoglycan 4 supplementation,” *Arthritis Rheum.*, vol. 64, no. 12, pp. 3963–3971, 2012.
[48] D. A. Swann, F. H. Silver, H. S. Slayter, W. Stafford, and E. Shore, “The molecular structure and lubricating activity of lubricin isolated from bovine and human synovial fluids,” *Biochem. J*, vol. 225, pp. 195–201, 1985.

[49] S. M. Iqbal *et al.*, “Lubricin/Proteoglycan 4 binds to and regulates the activity of toll-Like receptors in vitro,” *Sci. Rep.*, vol. 6, pp. 1–12, 2016.
[50] Selexis, “Selexis Lubris partnership advances difficult-to-express protein towards clinic,” *PR Newswire: News Distribution, Targetting and Monitoring*, 2012. .
[51] K. A. Waller *et al.*, “Intra-articular recombinant human proteoglycan 4 mitigates cartilage damage after destabilization of the medial meniscus in the Yucatan Minipig,” *Am. J. Sports Med.*, vol. 45, no. 7, pp. 1512–1521, 2017.
[52] A. Lambiase *et al.*, “A two-week, randomized, double-masked study to evaluate safety and efficacy of Lubricin (150 ug/mL) eye drops versus sodium hyaluronate (HA) 0.18% eye drops (Vismed (R)) in patients with moderate dry eye disease,” *Ocul. Surf.*, vol. 15, no. 1, pp. 77–87, 2017.
[53] R. Wang, “Cucurbit[n]uril host-guest complexes: the effects of inclusion on the chemical reactivity and spectroscopic properties of aromatic guest molecules,” Queen’s University, 2007.
[54] T. Steiner, “The hydrogen bond in the solid state,” *Angew. Chem. Int. Ed.*, vol. 41, pp. 48–76, 2002.
[55] J. P. Gallivan and D. A. Dougherty, “Cation-pi interactions in structural biology,” *Proc. Natl. Acad. Sci.*, vol. 96, no. 17, pp. 9459–9464, 1999.
[56] D. A. Dougherty, “Cation-pi interaction,” *Acc Chem Res*, vol. 46, no. 4, pp. 885–893, 2013.
[57] G. V. Oshovsky, D. N. Reinhoudt, and W. Verboom, “Supramolecular chemistry in water,” *Chem. Int. Ed.*, vol. 46, no. 14, pp. 2366–2393, 2007.
[58] B. D. E. Raynal, T. E. Hardingham, J. K. Sheehan, and D. J. Thornton, “Calcium-dependent protein interactions in MUC5B provide reversible cross-links in salivary mucus,” *J. Biol. Chem.*, vol. 278, no. 31, pp. 28703–28710, 2003.
[59] M. Ishibashi, K. Tsumoto, M. Tokunaga, D. Ejima, Y. Kita, and T. Arakawa, “Is arginine a protein-denaturant?,” *Protein Expr. Purif.*, vol. 42, pp. 1–6, 2005.
[60] T. Arakawa, K. Tsumoto, K. Nagase, and D. Ejima, “The effects of arginine on protein binding and elution in hydrophobic interaction and ion-exchange chromatography,” *Protein Expr. Purif.*, vol. 54, no. 1, pp. 110–116, 2007.
[61] D. Shukla and B. L. Trout, “Interaction of arginine with proteins and the mechanism by which it inhibits aggregation,” *J. Phys. Chem. B*, vol. 114, no. 42, pp. 13426–13438, 2010.
[62] T. Arakawa *et al.*, “Suppression of protein interactions by arginine: A proposed mechanism of the arginine effects,” *Biophys. Chem.*, vol. 127, pp. 1–8, 2007.
[63] V. Pascale, W. Pascale, V. Lavanga, V. Sansone, P. Ferrario, and V. De Gennaro Colonna, “L-arginine, asymmetric dimethylarginine, and symmetric dimethylarginine in plasma and synovial fluid of patients with knee osteoarthritis,” *Med. Sci. Monit.*, vol. 19, pp. 1057–1062, 2013.
[64] J. Kooyman, M. C. Alvarez-Veronesi, and T. A. Schmidt, “Cartilage Boundary Lubricating Properties of Native Proteoglycan 4 Purified from Normal Bovine Synovial Fluid,” *Trans Orthop Res Soc*, p. Poster 255, 2009.
[65] D. Harvey, “Chromatographic and Electrophoretic Methods,” in *Modern Analytic Chemistry*, 1st ed., McGraw Hill, 2000, pp. 597–598.
[66] C. Arndt, S. Koristka, H. Bartsch, and M. Bachmann, “Native polyacrylamie gels,” in *Protein electrophoresis: methods and protocols*, vol. 536, B. T. Kurien and R. H. Scofield, Eds. Oklahoma City: Humana Press, 2009, pp. 557–571.

[67] S. Abubacker, D. Ponjevic, H. O. Ham, P. B. Messersmith, J. R. Matyas, and T. A. Schmidt, “Effect of disulfide bonding and multimerization on proteoglycan 4′s cartilage boundary lubricating ability and adsorption,” *Connect. Tissue Res.*, vol. 57, no. 2, pp. 113–123, 2016.
[68] I. Puskás, M. Schrott, M. Malanga, and L. Szente, “Characterization and control of the aggregation behavior of cyclodextrins,” *J. Incl. Phenom. Macrocycl. Chem.*, vol. 75, no. 3–4, pp. 269–276, 2013.
[69] Y. Li, V. Lubchenko, and P. G. Vekilov, “The use of dynamic light scattering and Brownian microscopy to characterize protein aggregation,” *Rev. Sci. Instrum.*, vol. 82, no. 5, 2011.
[70] M. Kaszuba, D. McKnight, M. T. Connah, F. K. McNeil-Watson, and U. Nobbmann, “Measuring sub nanometre sizes using dynamic light scattering,” *J. Nanoparticle Res.*, vol. 10, no. 5, pp. 823–829, 2008.
[71] A. Hawe, W. L. Hulse, W. Jiskoot, and R. T. Forbes, “Taylor dispersion analysis compared to dynamic light scattering for the size analysis of therapeutic peptides and proteins and their aggregates,” *Pharm. Res.*, vol. 28, no. 9, pp. 2302–2310, 2011.
[72] J. Lim, S. P. Yeap, H. X. Che, and S. C. Low, “Characterization of magnetic nanoparticle by dynamic light scattering,” *Nanoscale Res. Lett.*, vol. 8, no. 1, p. 381, 2013.
[73] M. G. Rasteiro, C. C. Lemos, and A. Vasquez, “Nanoparticle characterization by PCS: The analysis of bimodal distributions,” *Part. Sci. Technol.*, vol. 26, no. 5, pp. 413–437, 2008.
[74] G. W. Stachowiak and A. W. Batchelor, *Engineering Tribology*, 4th ed. Elsevier Inc, 2014.
[75] D. Dowson, “Bio-tribology,” *Faraday Discuss.*, vol. 156, pp. 9–30, 2012.
[76] T. Crouzier *et al.*, “Modulating Mucin Hydration and Lubrication by Deglycosylation and Polyethylene Glycol Binding,” *Adv. Mater. Interfaces*, vol. 2, no. 18, pp. 1–7, 2015.
[77] G. W. Greene, X. Banquy, D. W. Lee, D. D. Lowrey, J. Yu, and J. N. Israelachvili, “Adaptive mechanically controlled lubrication mechanism found in articular joints,” *Proc. Natl. Acad. Sci.*, vol. 108, no. 13, pp. 5255–5259, 2011.
[78] G. D. Jay, “Characterization of a bovine synovial fluid lubricating factor. I. Chemical, surface activity and lubricating properties,” *Connect. Tissue Res.*, vol. 28, no. 1–2, pp. 71–88, 1992.
[79] S. Abubacker, A. Mcpeak, S. G. Dorosz, P. Egberts, and T. A. Schmidt, “Effect of counterface on cartilage boundary lubricating ability by proteoglycan 4 and hyaluronan: Cartilage-glass versus cartilage-cartilage,” *J. Orthop. Res.*, pp. 1–9, 2018.
[80] J. H. Zar, *Biostatistical Analysis*, Fourth. Upper Saddle River, N.J.: Prentice Hall, 1998.
[81] Y. Bai, Q. Luo, and J. Liu, “Protein self-assembly: Via supramolecular strategies,” *Chem. Soc. Rev.*, vol. 45, no. 10, pp. 2756–2767, 2016.
[82] M. C. Alvarez-Veronesi, J. Kooyman, and T. A. Schmidt, “Synthesis of Proteoglycan 4 (PRG4) Disulfide-Bonded Multimers by Chondrocytes in Cartilage Explants.,” in *Trans Orthop Res Soc*, 2010, p. 850.
[83] Z. Hong, B. Chasan, R. Bansil, B. S. Turner, K. R. Bhaskar, and N. H. Afdhal, “Atomic force microscopy reveals aggregation of gastric mucin at low pH,” *Biomacromolecules*, vol. 6, no. 6, pp. 3458–3466, 2005.
[84] B. Zappone, G. W. Greene, E. Oroudjev, G. D. Jay, and J. N. Israelachvili, “Molecular aspects of boundary lubrication by human lubricin: effect of disulfide bonds and

enzymatic digestion," *Langmuir*, vol. 24, no. 4, pp. 1495–1508, 2008.
[85] B. Lorber, F. Fischer, M. Bailly, H. Roy, and D. Kern, "Protein analysis by dynamic light scattering: methods and techniques for students," *Biochem. Mol. Biol. Educ.*, vol. 40, no. 6, pp. 372–382, 2012.
[86] V. L. Thomas, B. a Sanford, and M. a Ramsay, "Calcium- and mucin-binding proteins of staphylococci.," *J. Gen. Microbiol.*, vol. 139, no. 3, pp. 623–629, 1993.
[87] J. Seror, L. Zhu, R. Goldberg, A. J. Day, and J. Klein, "Supramolecular synergy in the boundary lubrication of synovial joints," *Nat. Commun.*, vol. 6, pp. 1–7, 2015.
[88] T. E. Ludwig, M. M. Hunter, and T. A. Schmidt, "Cartilage boundary lubrication synergism is mediated by hyaluronan concentration and PRG4 concentration and structure.," *BMC Musculoskelet. Disord.*, vol. 16, no. 1, p. 386, 2015.
[89] A. Morin, "Biophysical evidence for a molecular interaction between proteoglycan 4 and hyaluronan in solution: effect of exposure to a zwitterionic detergent on cartilage boundary lubricating function," University of Calgary, 2016.

Appendix

Copyright permission for the use of Figure 1-1.

Table of Contents

1. Comments

- Book review
- Open Access

Mow VC, Huiskes R: Basic Orthopaedic Biomechanics and Mechano-Biology

3rd edition. Philadelphia: Lippincott Williams & Wilkins; 2005. ISBN 0-7817-3933-0. xvi+720 pages. US$110

- Eduardo Abreu[1] Email author

BioMedical Engineering OnLine2005**4**:28

[illegible]

[illegible]

- [illegible]
- [illegible]
- [illegible]

[illegible]

[illegible]

[

Copy right permission for the use of Figure 1-2.

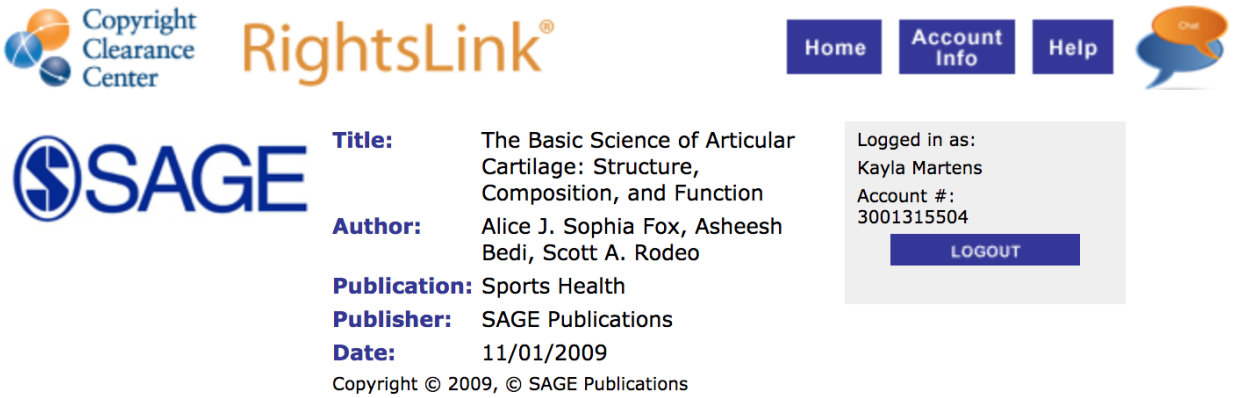

Copyright permission for the use of Figure 1-3.

Friday, September 14, 2018 at 5:47:59 PM Mountain Daylight Time

Subject: Thank you for your order with RightsLink / Elsevier
Date: Thursday, August 9, 2018 at 7:52:58 PM Mountain Daylight Time
From: no-reply@copyright.com
To: Kayla Martens

Thank you for your order!

Dear Ms. Kayla Martens,

Thank you for placing your order through Copyright Clearance Center's RightsLink® service.

Order Summary

Licensee:	Ms. Kayla Martens
Order Date:	Aug 9, 2018
Order Number:	4405090367827
Publication:	Current Opinion in Colloid & Interface Science
Title:	Molecular mechanisms of aqueous boundary lubrication by mucinous glycoproteins
Type of Use:	reuse in a thesis/dissertation
Order Total:	0.00 USD

View or print complete details of your order and the publisher's terms and conditions.

Sincerely,

Copyright Clearance Center

Tel: +1-855-239-3415 / +1-978-646-2777
customercare@copyright.com
https://myaccount.copyright.com

Copyright Clearance Center RightsLink®

Copyright permission for the use of Figure 1-4.

Friday, September 14, 2018 at 5:49:30 PM Mountain Daylight Time

Subject: Thank you for your order with RightsLink / Elsevier
Date: Thursday, August 9, 2018 at 9:19:01 PM Mountain Daylight Time
From: no-reply@copyright.com
To: Kayla Martens

Thank you for your order!

Dear Ms. Kayla Martens,

Thank you for placing your order through Copyright Clearance Center's RightsLink® service.

Order Summary

Licensee:	Ms. Kayla Martens
Order Date:	Aug 9, 2018
Order Number:	4405120995035
Publication:	Matrix Biology
Title:	The biology of Lubricin: Near frictionless joint motion
Type of Use:	reuse in a thesis/dissertation
Order Total:	0.00 USD

View or print complete details of your order and the publisher's terms and conditions.

Sincerely,

Copyright Clearance Center

Tel: +1-855-239-3415 / +1-978-646-2777
customercare@copyright.com
https://myaccount.copyright.com

Copyright Clearance Center RightsLink®

Copyright permission for the use of Figure 1-5.

Copyright Clearance Center

Confirmation Number: 11748301
Order Date: 09/13/2018

Customer Information

Customer: Kayla Martens
Account Number: 3001315504
Organization: Kayla Martens
Email: kayla.martens1@ucalgary.ca
Phone: +1 (905) 449-4021
Payment Method: Invoice

This is not an invoice

Order Details

JOURNAL OF CLINICAL INVESTIGATION. ONLINE

Billing Status: **N/A**

Order detail ID:	71552185
ISSN:	1558-8238
Publication Type:	e-Journal
Volume:	
Issue:	
Start page:	
Publisher:	AMERICAN SOCIETY FOR CLINICAL INVESTIGATION
Author/Editor:	American Society for Clinical Investigation

Permission Status: Granted
Permission type: Republish or display content
Type of use: Thesis/Dissertation
Order License Id: 4427170401858

Requestor type	Academic institution
Format	Electronic
Portion	image/photo
Number of images/photos requested	1
The requesting person/organization	Kayla Martens/University of calgary
Title or numeric reference of the portion(s)	Chapter 1, Figure 1-5
Title of the article or chapter the portion is from	The secreted glycoprotein lubricin protects cartilage surfaces and inhibits synovial cell overgrowth
Editor of portion(s)	N/A
Author of portion(s)	David K. Rhee, Jose Marcelino, MacArthur Baker, Yaoqin Gong, Patrick Smits, Veronique Lefebvre, Gregory Jay, Matthew Stewart, Hongwei Wang, Matthew Warman, John Carpten
Volume of serial or monograph	115
Page range of portion	623
Publication date of portion	2005
Rights for	Main product
Duration of use	

	Life of current and all future editions
Creation of copies for the disabled	no
With minor editing privileges	no
For distribution to	Canada
In the following language(s)	Original language of publication
With incidental promotional use	no
Lifetime unit quantity of new product	Up to 499
Title	Characterization of Proteoglycan 4 Supramolecular Structure and its Effect on Lubricating Function
Instructor name	n/a
Institution name	n/a
Expected presentation date	Sep 2018

Note: This item was invoiced separately through our **RightsLink service.** More info **$ 0.00**

Total order items: 1 **Order Total: $0.00**

Copyright permission for the use of Figure 1-6.

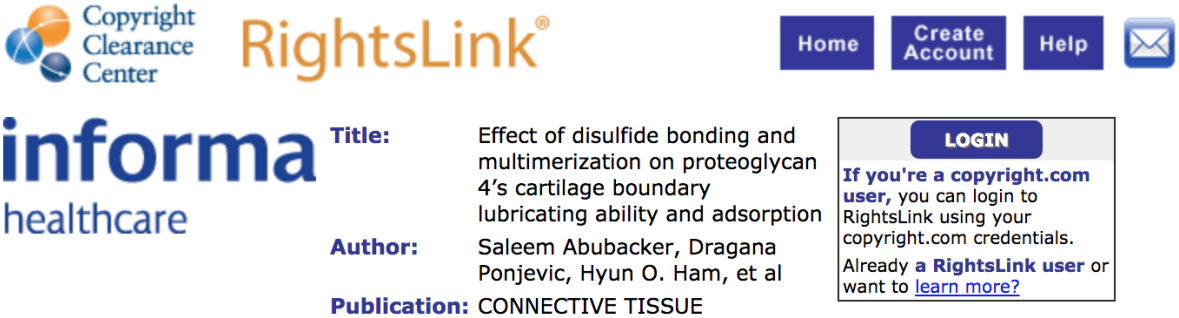

Thesis/Dissertation Reuse Request

Taylor & Francis is pleased to offer reuses of its content for a thesis or dissertation free of charge contingent on resubmission of permission request if work is published.

BACK CLOSE WINDOW

Copyright permission for the use of Figure 1-7.

Copyright Clearance Center

Confirmation Number: 11747691
Order Date: 09/11/2018

Customer Information

Customer: Kayla Martens
Account Number: 3001315504
Organization: Kayla Martens
Email: kayla.martens1@ucalgary.ca
Phone: +1 (905) 449-4021
Payment Method: Invoice

This is not an invoice

Order Details

Soft matter

Billing Status: **N/A**

Order detail ID:	71542216
ISSN:	1744-6848
Publication Type:	e-Journal
Volume:	
Issue:	
Start page:	
Publisher:	ROYAL SOCIETY OF CHEMISTRY
Author/Editor:	Royal Society of Chemistry (Great Britain)

Permission Status: Granted
Permission type: Republish or display content
Type of use: Thesis/Dissertation
Order License Id: 4426190942928

Requestor type	Academic institution
Format	Electronic
Portion	image/photo
Number of images/photos requested	1
The requesting person/organization	Kayla Martens/University of calgary
Title or numeric reference of the portion(s)	Chapter 1, Figure 1-7
Title of the article or chapter the portion is from	Characterization of proteoglycan 4 Supramolecular Structure and its Effect on Lubricating Function
Editor of portion(s)	N/A
Author of portion(s)	N/A
Volume of serial or monograph	N/A
Page range of portion	19
Publication date of portion	2018
Rights for	Main product
Duration of use	Life of current edition
Creation of copies for the disabled	no
With minor editing privileges	no
For distribution to	Canada

In the following language(s)	Original language of publication
With incidental promotional use	no
Lifetime unit quantity of new product	Up to 499
Title	Characterization of Proteoglycan 4 Supramolecular Structure and its Effect on Lubricating Function
Instructor name	n/a
Institution name	n/a
Expected presentation date	Sep 2018

Note: This item was invoiced separately through our **RightsLink service.** More info **$ 0.00**

Total order items: 1 **Order Total: $0.00**

Copyright permission for the use of Figure 2-1.

Friday, September 14, 2018 at 5:47:01 PM Mountain Daylight Time

Subject: Thank you for your order with RightsLink / AIP Publishing
Date: Monday, July 30, 2018 at 11:59:06 AM Mountain Daylight Time
From: no-reply@copyright.com
To: Kayla Martens

Thank you for your order!

Dear Ms. Kayla Martens,

Thank you for placing your order through Copyright Clearance Center's RightsLink® service.

Order Summary

Licensee:	Ms. Kayla Martens
Order Date:	Jul 30, 2018
Order Number:	4398900664077
Publication:	Review of Scientific Instruments
Title:	Adapting a commercial shear rheometer for applications in cartilage research
Type of Use:	Thesis/Dissertation
Order Total:	0.00 USD

View or print complete details of your order and the publisher's terms and conditions.

Sincerely,

Copyright Clearance Center

Tel: +1-855-239-3415 / +1-978-646-2777
customercare@copyright.com
https://myaccount.copyright.com

Copyright Clearance Center RightsLink®

Copyright for permission for the use of Figure 2-2.

Friday, September 14, 2018 at 5:45:02 PM Mountain Daylight Time

Subject: Thank you for your order with RightsLink / Elsevier
Date: Monday, July 30, 2018 at 11:51:12 AM Mountain Daylight Time
From: no-reply@copyright.com
To: Kayla Martens

Thank you for your order!

Dear Ms. Kayla Martens,

Thank you for placing your order through Copyright Clearance Center's RightsLink® service.

Order Summary

Licensee:	Ms. Kayla Martens
Order Date:	Jul 30, 2018
Order Number:	4398900190153
Publication:	Osteoarthritis and Cartilage
Title:	Effect of synovial fluid on boundary lubrication of articular cartilage
Type of Use:	reuse in a thesis/dissertation
Order Total:	0.00 CAD

View or print complete details of your order and the publisher's terms and conditions.

Sincerely,

Copyright Clearance Center

Tel: +1-855-239-3415 / +1-978-646-2777
customercare@copyright.com
https://myaccount.copyright.com

Copyright Clearance Center RightsLink®